Titanium dioxide nanoparticles enhance macrophage activation by LPS through a TLR4-dependent intracellular pathway

Titanium dioxide nanoparticles enhance macrophage activation by LPS through a TLR4-dependent intracellular pathway

Journal:	*Toxicology Research*
Manuscript ID:	TX-ART-11-2014-000193.R1
Article Type:	Paper
Date Submitted by the Author:	n/a
Complete List of Authors:	Bianchi, Massimiliano; University of Parma, Allegri, Manfredi; University of Parma, Costa, Anna; CNR, ISTEC Blosi, Magda; ISTEC CNR, Institute of Science and Technology for Ceramics Gardini, Davide; CNR, ISTEC Del Pivo, Camilla; CNR, ISTEC Prina Mello, Adriele; Trinity College Dublin, CRANN Di Cristo, Luisana; University of Parma, Bussolati, Ovidio; University of Parma, Dept. SBiBiT Bergamaschi, Enrico; University of Parma, Dept. of Clinical and Experimental Medicine

Dear prof. van Schooten:

The revised version of the ms. “Titanium dioxide nanoparticles enhance macrophage activation by LPS via a TLR4-dependent intracellular pathway “ by Bianchi et al.(TX-ART-11-2014-000193) is submitted to your consideration for publication on Toxicology Research.

The comments by the Reviewers have been addressed as follows:

Reviewer 1

1) The PCR tests were indeed real time experiments. Thus, the values reported in Figs. 1, 2, 3 represent a quantitative assessment of the levels of Nos2 and Ptgs2 expressed relatively to Gapdh following the method of Bustin et al. (ref. 28). We apologize for the inadequate abbreviation “RT-PCR” that has misled the Reviewer. The sub-title of section 2.5 has been now modified in “Real time Polymerase chain reaction” (p. 10).
2) The ms. language has been thoroughly revised throughout.

Reviewer 2

1) We adopted BSA as a dispersant agent because this study was a part of a cooperative project (EU FP Sanowork) in which all the participants agreed on a shared experimental protocol. In particular, the conditions adopted for the preparation of stock suspensions (0.05% BSA in Ca and Mg free Phosphate Buffered Saline) were a modification of the protocol adopted in the Nanogenotox project. However, stock were diluted 100-fold in complete medium for cell exposure. Thus, wet characterization was performed either in water or in medium so as to approximate the real conditions present during the experimental exposure. This rationale has been given in the text of the revised version (p. 7).
2) Although our study specifically concerns LPS and TLR4, we are well aware of the possible general implications of our findings for other TLR ligands (see Conclusions). To address the request of the Reviewer we have added an explicatory sentence at the beginning of section 3.5 (p. 19) and have modified the last sentence of the Discussion (p. 23).

Moreover, the ms. has been completely revised so as to amend some mistakes present in the text, in the axis legends of Figs. 1 and 2, and in the cartoon reported in Fig. 8.

We hope that our manuscript now fits the requirements to be accepted for publication on Toxicology Research and wish to thank you and the Reviewers for the interest in our work.

Sincerely Yours,

Ovidio Bussolati

Titanium dioxide nanoparticles enhance macrophage activation by LPS through a TLR4-dependent intracellular pathway

Massimiliano G. Bianchi[a§], Manfredi Allegri[b§], Anna L. Costa[c], Magda Blosi[c], Davide Gardini[c], Camilla Del Pivo[c], Adriele Prina-Mello[d], Luisana Di Cristo[a], Ovidio Bussolati[b*], Enrico Bergamaschi[a]

[a]Unit of Occupational Medicine, Department of Clinical and Experimental Medicine, University of Parma, 43026 Parma, Italy

[b]Unit of General Pathology, Department of Biomedical, Biotechnological and Translational Sciences, University of Parma, 43025 Parma, Italy

[c]Institute of Science and Technology for Ceramics (CNR-ISTEC), National Research Council of Italy, 48018 Faenza(RA), Italy

[d] Centre for Research on Adaptive Nanostructures and Nanodevices (CRANN) and School of Medicine, Trinity College Dublin, Dublin

[§]These authors contributed equally to this work

*Corresponding Author:
Ovidio Bussolati
Unit of General Pathology
Department of Biomedical, Biotechnological and Translational Sciences (SBiBiT)
University of Parma
43025 Parma
Italy
Tel +39 0521033783
ovidio.bussolati@unipr.it

Abstract

Although causing moderate cytotoxicity and inflammatory effects, TiO_2 nanoparticles (NP) are considered relatively safe materials. However, it is known that TiO_2 NP bind bioactive environmental contaminants, such as bacterial lipopolysaccharide (LPS, endotoxin), and it is possible that this interaction leads to increased biological activity. In this report we have investigated the pro-inflammatory responses of Raw264.7 murine macrophages exposed to two preparations of TiO_2 NP, co-administered with LPS. The simultaneous exposure to NP and LPS produced marked increases in *Nos2* mRNA, Nos2 protein and medium nitrite concentration (an indicator of NO production) well beyond the levels observed with LPS or TiO_2 NP alone. TiO_2 NP also synergized LPS effects on *Ptgs2* expression and cytokine secretion. The cytoskeletal drug cytochalasin B lowered the amount of NP internalized by the cells and suppressed the synergy between TiO_2 NP and LPS on NO production and cytokine secretion. Pre-treatment with the TLR4 inhibitors polymyxin B and CLI-095 abolished the synergy that was also partially hampered by the inhibition of p38 MAPK, but not of ERK1/2. Moreover, p38 phosphorylation was synergistically enhanced by the combined treatment at 6h of incubation. It is concluded that TiO_2 NP enhance macrophage activation by LPS via a TLR4-dependent mechanism that involves p38 and is mainly triggered from an intracellular site. These findings suggest that the simultaneous exposure to LPS and TiO_2 NP may exacerbate the inflammatory response *in vivo*.

Abbreviations

CLI-095, Ethyl (6R)-6-[N-(2-Chloro-4-fluorophenyl)sulfamoyl]cyclohex-1-ene-1-carboxylate; DRAQ5®, 1,5-bis[2-(di-methylamino) ethyl]amino-4, 8-dihydroxyanthracene-9,10-dione; NP, nanoparticles; SB203580, 4-(4-fluorophenyl)-2-(4-methylsulfinylphenyl)-5-(4-pyridyl)-imidazole; PAMP, Pathogen-Associated Molecular Pattern; TBS, Tris-Buffered saline; TLR4, Toll-like receptor 4; U0126, 1,4-diamino-2,3-dicyano-1,4-bis[2-aminophenylthio] butadiene.

Table of contents entry

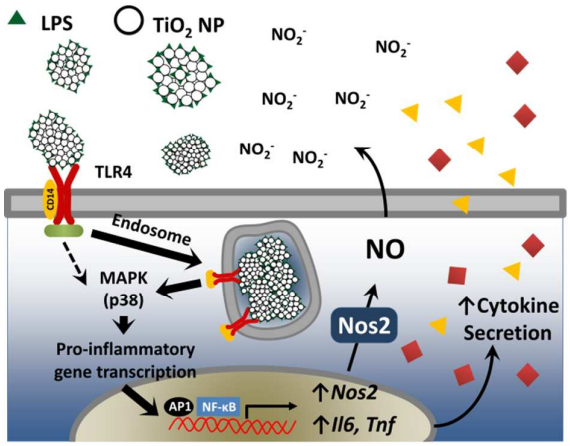

TiO_2 nanoparticles enhance LPS-dependent NO production and cytokine secretion through a mechanism that involves TLR4-mediated p38-signalling and requires phagocytosis

1. Introduction

Lipopolysaccharides (LPS, endotoxins) are large, heat-stable molecules (molecular weight: 200 to 1000 kDa) from the outer membrane of Gram-negative bacteria, consisting of a polysaccharidic moiety (O domain) and a bioactive lipid part, known as lipid A, responsible for their toxicity. LPS are Pathogen-Associated Molecular Patterns (PAMPs), acting as strong macrophage activators, and their effects range from airway disease, to fever, hypotension, septic shock, depending on the administration route and dose. In mammals, including man, most of the toxic/inflammatory effects of LPS and, in particular, all those based on transcriptional mechanisms, are mediated through the Toll-like Receptor 4 (TLR4) signalling pathway.[1] The activation of innate immune cells, such as monocytes and macrophages, by LPS through TLR4 is a major step of the defensive inflammatory reaction against bacteria and is initiated in different cellular locations, triggering distinct transduction pathways, first at the plasma membrane and later from an endosomal compartment.[2] LPS-stimulated cells produce a variety of inflammatory factors, such as tumor necrosis factor-α (TNF-α) and interleukin-6 (IL-6), and secrete nitric oxide (NO), a short-lived free radical, which mediates many biological functions such as host defence, neurotransmission, neurotoxicity and vasodilation.

Among metal oxide nanoparticles (NP), titanium dioxide (TiO_2) NP occupy a prominent position with a large use as sun blocking filters in cosmetics and, due to their photocatalytic activity, as self-cleaning, antibacterial and anti-polluting coatings onto different substrates. The increasing use of TiO_2 NP has promoted their large-scale production and, at the same time, has led to a growing concern about the risks to human health, in particular for workers regularly exposed, and to the environment. Indeed, although bulk TiO_2 has been classified as a biologically inert material for humans and animals,[3] evidence has been repeatedly reported on TiO_2 NP toxicity in several animal models *in vivo*, with inflammation,[4] enhanced proliferation of pulmonary cells at relatively high doses,[5,6] and carcinogenicity.[7] Since the respiratory tract represents the main route of NP access to the body, especially in occupational settings, the above studies have been carried out through

inhalation or tracheal instillation. However, also systemic administration is linked to inflammatory changes in lungs.[8]

The interaction between LPS and TiO_2 NP may modify NP toxicity *in vivo*. For instance, Moon et al.[9] have demonstrated that TiO_2 NP are able to induce acute inflammation in mice causing more evident effects if animals were primed by a treatment with LPS. Possible interactions between LPS and nanomaterials are not limited to TiO_2 NP since other engineered nanomaterials may be indeed contaminated with bacterial endotoxin or other PAMPs. For instance, LPS may enhance the oxidative stress induced by amorphous silica NPs to initiate cytotoxicity,[10] and carbon nanotubes promote NLRP3 inflammasome activation in synergy with TLR ligands.[11]

Biological effects of TiO_2 NP have also been investigated in a number of *in vitro* studies. Several reports have demonstrated that TiO_2 NP generate ROS[12-14] and induce genotoxicity,[12-15] but only relatively mild acute cytotoxicity in macrophages and airway epithelial cells.[16-19]

The possibility that the assessment of NP toxicity *in vitro* may be influenced by their contamination with bio-active molecules, and, in particular by LPS, has been debated.[20] Indeed, previous studies performed with fine TiO_2 particles and LPS suggested that the material was able to bind LPS and that the interaction enhanced the biological effects of the endotoxin.[21, 22] LPS binding to nanosized TiO_2 is expected to be much higher due to higher surface area of NP compared to fine particles. In a recent study, Jiang reported that the binding between TiO_2 NP and LPS is relatively strong and does not involve the lipid A but the polysaccharide moiety.[23] As a consequence, the interaction between LPS and TiO_2 NP should not prevent the binding between the endotoxin and TLR4. This hypothesis is consistent with the findings by Smulders et al.[24] who, while evaluating different test methods to detect nanomaterial contamination with LPS, have reported a synergistic TLR4 activation by LPS and several types of NP, and in particular of TiO_2 NP, in a mammalian cell model transfected with the receptor gene.

Using Raw264.7 cells, a macrophage line endowed with high endogenous TLR4 expression and widely adopted in nanotoxicological studies , the present investigation concerns the synergistic effect of LPS and TiO_2 NP on inflammatory endpoints and the role played therein by TLR4.

2. Experimental

2.1 Preparation and dispersion of NP

Experiments presented in this study were performed on two preparations of TiO_2 NP of industrial origin. Aeroxide® P25 NP (anatase/rutile 83/17, produced through the flame hydrolysis Aerosil® process) was purchased from Evonik Degussa GmbH, Germany. Selected experiments were also performed with a colloidal suspension of TiO_2 NP (NAMA41®, 6 wt%, anatase/brookite 84/16, obtained through dispersion in water), provided by Colorobbia Holding S.p.A., Italy.

For experiments, NP were dispersed according to a protocol adopted in the EU FP7 Project SANOWORK. Briefly, Aeroxide® P25 NP were heated at 230°C for 3h to ensure endotoxin elimination.[19,25] NP were then suspended in a sterile-filtered solution of 0.05% Bovine Serum Albumin (Sigma Aldrich, Milan, Italy, cat. A9418) in Phosphate Buffered Saline (PBS) without calcium and magnesium to obtain a 100x stock suspension of the highest dose tested (80 $\mu g/cm^2$, corresponding to 128 µg/ml). Appropriate dilutions in 0.05% BSA in PBS were performed to obtain 100x stock suspensions of the other doses. For the preparation of NAMA41® stock solution, the percent of BSA in PBS was corrected in order to reach a final concentration of 0.05%. After vortexing (30 s), sonication (10 min), and a further brief vortexing. the stocks were subsequently diluted in the same solvent to obtain the other 100X stocks. The stock solutions were made fresh for each experiment.

2.2 Characterization of TiO_2 NP

The physico-chemical characterization of the TiO_2 NP when interacting with the biological environment were carried out adopting the same conditions adopted for the *in vitro* cellular tests reported below (e.g., time, temperature, doses). In particular, given that the stock suspensions were 100-fold diluted in medium for cell exposure, the characterization was performed both in water and in complete growth medium.

Particle size distribution was evaluated by dynamic light scattering (DLS) technique assessing the hydrodynamic diameter of the dispersed NPs.

Similarly, a laser scattering technique was used to assess the ζ potential as expression of surface charge of TiO_2 NPs and of their colloidal stability in the selected aqueous medium. For both DLS and ζ potential measurements, the stock solutions (10 mg/ml) were sonicated for 15 minutes and diluted to 128 μg/ml, both in deionized water and in complete medium (Dulbecco's modified Eagle's medium (DMEM), Euroclone, code n° ECB7501L, Pero, Milan, Italy). Standard polystyrene cuvette and folded capillary cell DTS 1070 were used for size and zeta potential measurements, respectively.

Particle size and ζ potential of dispersed particles were measured by applying Dynamic Light Scattering (DLS) and Laser Doppler Velocimetry (LDV) techniques, respectively, using ZetasizerNano ZS (Malvern Instruments, UK). For the evaluation of particle size, data were recorded at 25 ± 1°C, in a backscattering detection mode (scattering angle of 173°). Each result corresponds to the average of five consecutive measurements and each measurement is the average of 15 analyses. The instrument measures the hydrodynamic diameter that is a diameter that includes the coordination sphere and the species adsorbed on the particle surface such as stabilizers, surfactants and so forth. DLS analysis provides also a polydispersity index (PDI), which is a number ranging from 0 to 1 useful to quantify the colloidal dispersion degree: samples with PDI close to 0 are considered monodispersed. Size data are calculated directly from correlation function (Cumulants analysis for z-average diameter and polydispersity index; CONTIN analysis for intensity size distribution).

For the evaluation of ζ potential the system records light scattered at an angle of 13°, determining an electrophoretic mobility. The Smoluchowski approximation was applied to calculate ζ potential from the mobility.

The specific surface area (SSA) was determined by BET single point method (Sorpty 1750, Carlo Erba, Milano, Italy). For spherical shape particles it is possible to correlate specific surface area to diameter by a simple geometric relationship.[26]

$$d = \frac{6}{\rho \, X \, SSA}$$

where:

SSA: specific surface area (m^2/g)

d = particle mean diameter (μm)

ρ = powder density (g/cm^3)

Applying this relationship it was possible to calculate the particle mean diameter from SSA and to compare it with the hydrodynamic diameter obtained by DLS.

2.3 Cell culture and experimental treatments

Murine peritoneal monocyte-macrophage cells (Raw264.7 line) were obtained from the Cell Bank of the Istituto Zooprofilattico della Lombardia e dell'Emilia (Brescia, Italy). Raw264.7 cells were cultured in Dulbecco's modified Eagle's medium (DMEM) supplemented with 10% FBS, 4mM glutamine, streptomycin (100 μg/ml) and penicillin (100 U/ml). Cells were routinely cultured in 10-cm diameter dishes maintained in a humidified atmosphere of 5% CO_2 in air. For experiments, cells were seeded in complete growth medium in 96-well plates, at a density of 30×10^3cells/well or in 24-well plates at a density of $15x10^4$ cells/well. Cell growth medium was replaced, 24h after cell seeding, with fresh medium supplemented with TiO_2 NP at the doses indicated for each experiment in the presence or in the absence of LPS (from *E.coli*, O55:B5 serotype, Sigma-Aldrich, Milan, Italy) at a concentration of 1 ng/ml or 10 ng/ml (from 100X stock solutions in DMEM). In all the experiments, vehicle (PBS + BSA) was added to the control.

For experiments in which inhibitors of macrophage activation were used, compounds were added 1h before the exposure to LPS and/or NP and maintained throughout the experiment. The selected inhibitors were: Ethyl (6R)-6-[N-(2-Chloro-4-fluorophenyl)sulfamoyl]cyclohex-1-ene-1-carboxylate (CLI-095, 1 μg/ml, from a stock solution of 10 μg/ml in DMEM, InvivoGen, San Diego, CA, USA); polymyxin B (50 μg/ml, from a stock solution of 500 μg/ml in DMEM, InvivoGen); cytochalasin B (5 μg/ml, from a stock solution of 50 μg/ml in DMEM; Sigma-Aldrich), 1,4-diamino-2,3-dicyano-1,4-bis[2-aminophenylthio] butadiene (U0126, 1 μM, from a stock solution of 10 mM in DMSO, Calbiochem, Merck Millipore, Darmstadt, Germany); 4-(4-fluorophenyl)-2-(4-methylsulfinylphenyl)-5-(4-pyridyl)-imidazole (SB203580, 2 μM, from a stock solution of 10 mM in DMSO, Calbiochem).

2.4 Cell viability

Cell viability was assessed with the resazurin method.[27] Resazurin is a non-fluorescent molecule which is converted by intracellular enzymes in the fluorescent compound resorufin (λ_{em} = 572 nm). After 48h of incubation in the presence of TiO_2 NP (dose range 10 - 80 μg/cm^2), cell viability was tested replacing medium with a solution of resazurin (44 μM, Sigma-Aldrich) in serum-free DMEM. After 20 min, fluorescence was measured at 572 nm with a multimode plate reader Perkin Elmer Enspire (Waltham, MA, USA). Since nanomaterials could interfere with cytotoxicity tests, a preliminary test was performed incubating the dye with TiO_2 NP only (128 μg/ml) and then measuring fluorescence. No fluorescence signal was detected above background.

2.5 Real-time polymerase chain reaction

Total RNA was isolated with GenElute Mammalian Total RNA Miniprep Kit (Sigma–Aldrich). After reverse transcription, aliquots of cDNA from each sample were amplified in a total volume of 25 μl with Go Taq PCR Master Mix (Promega, Italia, Milan, Italy), along with the forward and reverse primers (5 pmol each) reported in Table 1. Real-time PCR was performed in a 36-well

RotorGeneTM3000, version 5.0.60 (Corbett Research, Mortlake, Australia). For all the messengers to be quantified, each cycle consisted of a denaturation step at 95 °C for 20 s, followed by separate annealing (30s) and extension (30s) steps at a temperature characteristic for each pair of primers (Table 1). Fluorescence was monitored at the end of each extension step. Melting curve analysis was added at the end of each amplification cycle. The analysis of the data was made according to the relative standard curve method.[28] Expression data were reported as the ratio between each investigated mRNA and *Gapdh* mRNA.

2.6 Western blot

Cells were lysed in a buffer containing 20 mM Tris–HCl, pH 7.5, 150 mM NaCl, 1 mM EDTA, 1 mM EGTA, 1% Triton, 2.5 mM sodium pyrophosphate, 1 mM β-glycerophosphate, 1 mM Na_3VO_4, 1 mM NaF, 2 mM imidazole and a cocktail of protease inhibitors (Complete, Mini, EDTA-free, Roche, Monza, Italy). Lysates were transferred in Eppendorf tubes, sonicated for 15s and centrifuged at 12,000*g* for 20 min at 4°C. After quantification with the Bio-Rad protein assay, aliquots of proteins (30 µg) were mixed with Laemmli buffer 4× (250 mMTris–HCl, pH 6.8, 8% SDS, 40% glycerol, and 0.4M DTT), warmed at 95°C for 10 min and loaded on a 8% gel for SDS-PAGE. After electrophoresis, proteins were transferred to PVDF membranes (Immobilon-P, Millipore, Millipore Corporation, MA, USA). Non-specific binding sites were blocked with an incubation of 1h at room temperature in blocking solution (Western Blocking Reagent, Roche) diluted in TBS (Tris-Buffered saline, pH 7.5). The blots were then exposed at 4°C overnight to the following antibodies diluted in 5% BSA in TBST (Tween 100 0.1% in TBS): anti-Nos2 (rabbit polyclonal, 1:400, Santa Cruz Biotechnology, Santa Cruz, CA, USA); anti-phospho-p38 (rabbit polyclonal, 1:500, R&D Systems, Minneapolis, MN, USA); anti-p38, (rabbit polyclonal, 1:400, R&D Systems); anti-actin (mouse monoclonal, 1:4,000, Sigma-Aldrich); anti-tubulin (mouse monoclonal, 1:1,000, Sigma-Aldrich). After washing, the blots were exposed for 1 h at room temperature to HRP-conjugated anti-rabbit or anti-mouse antibodies (Cell Signaling Technology,

Danvers, MA, USA), diluted 1:20,000 in blocking solution. Immunoreactivity was visualized with Immobilon Western Chemiluminescent HRP Substrate (Millipore, Merck).

2.7 Nitrite production

Nitrite concentration in the culture media of Raw264.7 was determined through a fluorometric approach. The method is based on the production of the fluorescent molecule 1-(*H)*-naphthotriazole from 2,3-diaminonaphthalene (DAN, Invitrogen, Life Technologies, Monza, Italy) in an acid environment[29]. After 48 h of incubation with TiO_2 NP in the presence or in the absence of LPS, 100 µl of medium were transferred in black 96-well plates with a clear bottom (Corning, Cambridge, MA, USA). DAN (20 µl of a solution of 0.025 mg/ml in 0.31 M HCl) was then added and, after 10 min at room temperature, the reaction was stopped with 20 µl of 0.7 M NaOH. Standards were performed in the same medium from a solution of 1 mM sodium nitrite. Fluorescence was determined with a multimode plate reader Perkin Elmer Enspire.

2.8 Cytokine assays

TNF-α secretion in the culture media of Raw264.7 cells was determined with ELISA RayBio® kit (Ray Biotech, Norcross, GA, USA). After 48 hours of incubation under the conditions indicated for each experiment, 100 µl of medium were transferred in 96-well plates functionalized with anti-TNF-α antibody and incubated overnight at 4°C. Then, 100 µl of biotinylated antibody were added in each well and, after 1 h of incubation at RT, 100 µl of streptavidin solution were also added. After 45 min the samples were incubated with 100 µl of the TMB One Step Reagent contained in the kit solution and, after 30 min, reaction was stopped, and absorbance was immediately read at 450 nm with a multimode plate reader Perkin Elmer Enspire. Standards were performed from a solution of 50 ng/ml of recombinant TNF-α.

2.9 Confocal microscopy

Cells were seeded on four-chamber slides at a density of $15x10^4$ cells/cm^2 and treated after 24 h with TiO_2 NP at the dose of 10 μg/cm^2 in the presence or in the absence of 1 ng/ml LPS, with or without cytochalasin B (5 μg/ml). The incubation was prolonged for 24 h. 20 min before the end of exposure, cells were transferred in serum-free medium supplemented with CellTracker™ Red CMPTX (8 μM, Molecular Probes, Invitrogen) to label cytoplasm; in the last 5 min 1,5-bis[2-(di-methylamino)ethyl]amino-4, 8-dihydroxyanthracene-9,10-dione (DRAQ5®, 20 μM, Alexis Biochemicals, San Diego, CA, USA) was also added to the incubation medium to counterstain nuclei. At the end of the exposure, cell monolayers were rinsed twice in PBS and fixed with 3.7% paraformaldehyde at room temperature for 15 min. Specimens were then mounted on glass slides with fluorescence mounting medium (Dako Italia SpA, Milan, Italy) and imaged by confocal microscopy.

Confocal analysis was carried out with a LSM 510 Meta scan head integrated with an inverted microscope (Carl Zeiss, Jena, Germany). Samples were observed through a 63x (1.4 NA) oil objective. Image acquisition was carried out in multitrack mode, i.e. through consecutive and independent optical pathways. Excitation at 488 nm and reflectance were used to visualize TiO_2 NP; excitation at 543 nm and emission recorded through a 580-630 nm band pass barrier filter were used to visualize cytoplasm; excitation at 633 nm and emission through a 670 nm long pass filter were recorded to visualize the nucleus.

2.10 Statistics

Data are expressed as the mean ± standard deviation (mean ± SD). Statistical analyses were assessed by two-tail Student's t-test for unpaired data whenever not stated otherwise. Graph Pad Prism software version 4.00 (Graph Pad Software Inc., San Diego, CA) was used. Results were considered significant at $p < 0.05$.

3. Results

3.1 Physico-chemical characterization of TiO_2 NP

Physico-chemical properties of NAMA41® (spray dried) and Aeroxide® P25 are summarised in Table 2 whereas results of wet characterization (pH, ζ potential and mean hydrodynamic diameter by intensity) of their dispersions in deionized water or complete culture medium are reported in Table 3.

TiO_2 samples are comparable in phase distribution and density, although NAMA41® SSA_{BET} exceeds approximately two and a half times that of Aeroxide® P25, suggesting a bigger primary particle diameter for the latter preparation.

Both the samples showed a broad size distribution and a low colloidal stability, especially for Aeroxide® P25 NP that possess a lower ζ potential value in comparison to NAMA41® in all the dispersions tested. Sample stability strongly decreased passing from water dispersion at natural pH to culture medium, likely due to the increase of pH towards the isoelectric point that is 6.0-7.0 for titania[30]. In order to discriminate if colloidal stability was influenced by pH or by medium components, ζ potential and mean hydrodynamic diameter were compared in samples dispersed in water (at natural pH or at pH 7.5, roughly corresponding to the pH of culture medium) or in complete, serum-supplemented medium (Table 3, Supplementary Material, Figures S1-S3). The results showed that a strong destabilizing effect occurred at medium pH. This behaviour, more evident for NAMA41®, is explainable by considering that uncoated TiO_2 NP, passing from acidic to roughly neutral pH, crossed the isoelectric point and reverse ζ potential sign from positive to negative, with an expected destabilization of the sample, as demonstrated by the significant size increase and the absolute ζ potential value reduction. This trend was confirmed in medium, even if TiO_2 NP appeared to aggregate more in water at neutral pH than in complete medium, probably due to the protein corona stabilizing effect.[31] In water dispersion at pH 7.5 both TiO_2 samples showed a slightly negative ζ potentials which, in medium, became comparable and were compatible with the isoelectric point of BSA at the same pH (≅ 5).[32] Thus, the lower size increase and the levelling of ζ

potentials of the different TiO_2 NP dispersions tested detected in culture medium was consistent with protein adsorption on NP surfaces.

In order to discriminate between the contributions of medium components adsorbed onto TiO_2 NP surfaces or freely dispersed in the medium, samples were analyzed after ultrafiltration and redispersion in water. ζ potential values remained approximately the same (around -10 mV, data not shown), confirming that TiO_2 NP surfaces were coated by protein components, as suggested by the protein corona paradigm.[33]

Table 4 reports the amount of BSA (0.05% BSA concentration) normalized for the surface area of TiO_2 samples (at a dose of 80 μg/cm^2) derived from BET analysis and, hence, corresponding to the maximal theoretical free surface (see Table 2). The BSA amount normalized over powder surface area corresponds to 25.4 mg/m^2 and 65.1 mg/m^2 for NAMA41® and Aeroxide® P25, respectively. These data are consistent with the formation of BSA coating, since in all cases they are much higher than the minimum amount of BSA leading to surface saturation of TiO_2 NP under comparable conditions (0.04 mg/m^2,[32]). Analogously, Table 4 reports the amount of LPS (at a concentration of 1ng/ml) normalized for the surface of TiO_2 sample, in order to compare such value with the saturation threshold reported in literature (0.3 mg/m^2).[23]

3.2 Synergistic effects of TiO_2 NP and LPS on the expression of pro-inflammatory markers in macrophages

The effects of TiO_2 NP (dose range 10-80 μg/cm^2), alone or in combination with LPS (1 or 10 ng/ml), on the viability of Raw264.7 cells were tested by resazurin assay after a 48h-exposure (Supplementary Material, Figure S4). TiO_2 NP, alone or in the presence of LPS (1 ng/ml), did not significantly affect cell viability even at the highest dose tested. In the presence of 10 ng/ml LPS, a modest, but significant reduction of cell viability was detected at the highest dose of TiO_2 NP (80 μg/cm^2).

Figure 1A reports *Nos2* mRNA expression after 24h of treatment of Raw264.7 cells with 80 μg/cm^2 of TiO_2 NP alone or in combination with LPS (1 or 10 ng/ml). In cells treated with TiO_2 NP alone the messenger was much less induced compared with cells treated with 1 or 10 ng/ml LPS (2-fold induction vs. 5-fold induction with LPS 1 ng/ml and 30-fold induction with LPS 10 ng/ml). The simultaneous exposure to both LPS and TiO_2 NP induced *Nos2* at a higher level than LPS alone (16-fold with LPS 1 ng/ml and 55-fold with LPS 10 ng/ml).

The time dependency of the effect was studied at mRNA level (Figure 1B). After 6 h of exposure, a small increase in *Nos2* expression was detected in cells treated with TiO_2 NP alone, while *Nos2* mRNA was already markedly induced in cells treated with LPS or, simultaneously, with LPS and NP. *Nos2* expression increased in cells treated with TiO_2 NP up to 24h exposure, while it decreased between the 12h- and the 24h-time points in cells treated with LPS + TiO_2 NP or, more evidently, with LPS alone. Under this latter condition, *Nos2* was only slightly induced after 24h exposure compared with untreated cells (3-fold). On the contrary, at the same experimental time point, *Nos2* was still markedly induced compared with untreated control (19-fold increase) in cells treated with LPS and NP.

The synergistic effect of TiO_2 NP and LPS on *Nos2* gene expression was confirmed at protein level after a 48h exposure (Fig. 1C). The effect was typically dose-dependent, both in the absence and in the presence of LPS (1 ng/ml). In the absence of LPS, the lowest dose of NP able to induce Nos2 was 20 μg/cm^2, while 10 μg/cm^2 of TiO_2 NP were able to increase the expression of the protein in the presence of LPS (1 ng/ml).

The stimulation of *Nos2* expression was associated with the increase in NO production, as assessed from the nitrite concentration in the medium (Fig. 1D). Nitrite concentration was significantly enhanced after a 48h-exposure to TiO_2 NP (80 μg/cm^2) or LPS, with an evident synergistic effect. The maximal stimulation was recorded in the presence of 10 ng/ml LPS + TiO_2 NP, where a 33-fold increase in medium nitrites was detected compared with the matching control. Comparable effects

were observed with another murine macrophage line, MH-S, derived from alveolar macrophages (data not shown).

The synergy between TiO_2 NP and LPS was not limited to *Nos2* but involved also other inflammatory markers. *Ptgs2*, a pro-inflammatory LPS target gene which encodes for the inducible form of cyclooxygenase, Cox2, was only slightly induced by TiO_2 NP (80 μg/cm^2) alone, while LPS produced a 3-fold and 21-fold increase of *Ptgs2* mRNA at 1 ng/ml or 10 ng/ml LPS, respectively (Fig. 2A). The effect was much larger in cells co-treated with LPS and NP, with a 6-fold and a 43-fold induction at, respectively, 1 or 10 ng/ml.

The secretion of TNF-α (Fig. 2, Panel B) was detectable also in control, untreated Raw264.7 cultures and was significantly stimulated by TiO_2 NP (2-fold) or LPS alone (2-fold or 4.5-fold at 1 ng/ml or 10 ng/ml, respectively) and, at higher levels, by TiO_2 NP + LPS (4.5 or 7.5 at 1 or 10 ng/ml of LPS, respectively). Instead, IL-6 secretion (Panel C) was undetectable in untreated cells and in cells treated with TiO_2 NP alone but was readily stimulated by LPS at either 1 ng/ml (47±5 pg/ml) or, much more markedly, at 10 ng/ml (1100±40 pg/ml). Co-treatment with TiO_2 NP and LPS caused a marked, further increase in IL-6 secretion when compared with cells treated with LPS alone, either at 1 or at 10 ng/ml.

In the experiments described in Figure 3, the effects of Aeroxide P25® were compared with those of NAMA41®, a different preparation of titania of industrial origin. Also these NP are predominantly anatase but are synthesized through a different process (see Experimental). The effects on nitrite concentration in culture medium (Panel A), *Nos2* expression (Panel B), and cytokine secretion (Panel C) were comparable for both TiO_2 NP preparations. The effects of LPS and NAMA41® on NO production were clearly synergistic, as demonstrated with two-way ANOVA (Fig. 3A). Thus, the biological activity of the two titania in the presence of endotoxin was similar, as expected by their comparable capacity to bind LPS (see above, 3.1). These data indicate that enhancement of LPS effects is not a peculiar feature of Aeroxide P25®.

3.3 Sensitivity to cytoskeletal disorganization of LPS-dependent stimulation of NO production in the absence or in the presence of TiO_2 NP

The relevance of cytoskeletal integrity in the stimulation of NO production by LPS and TiO_2 NP was investigated in the experiments recounted in Figure 4. Although cytochalasin is known to inhibit LPS-dependent stimulation of NO production, interfering with Nos2 assembly on actin cytoskeleton,[34] the inhibition was not significant at 1 ng/ml of LPS, while the drug lowered NO production by roughly 30% in cells stimulated with 10 ng/ml of LPS. The inhibition was much more evident in cells treated with both LPS and TiO_2 NP, where cytochalasin lowered NO production by 60% (at LPS 1 ng/ml) by over 70% (at LPS 10 ng/ml). Therefore, while the simultaneous exposure to TiO_2 NP caused a marked increase in LPS-dependent stimulation of NO production in the absence of cytochalasin, the cytoskeletal drug completely suppressed the effect at 1 ng/ml LPS and severely lowered it at 10 ng/ml LPS (from +136% to +42%). Consistently, cytochalasin almost completely suppressed the synergistic effect of LPS (1 ng/ml) and TiO_2 NP on TNF-α secretion (from 4,525 ± 32 pg/ml to 1,424 ± 114 pg/ml; control 625 ± 120 pg/ml; n =3; $p<0.01$).

The effect of cytochalasin on the uptake of Aeroxide® P25 TiO_2 NP by Raw264.7 cells, incubated in the presence of LPS, was assessed in confocal microscopy (Figure 4, Panels B and C). In the absence of cytochalasin (Panel B) several cells exhibited large amounts of internalized NP, clustered in large agglomerates localized in discrete subcellular regions. NP were scarcely detectable in the extracellular space. Cytochalasin (Panel C) severely hampered TiO_2 NP internalization, and most TiO_2 NP were visualized outside the cells, in some cases close to the cell surface. Under both conditions, signals of internalized NP and cytoplasmic markers did not co-localize, suggesting that NP were sequestered in an intracellular compartment distinct from cytoplasm.

3.4 Role of MAPK activation in the effects of LPS and TiO_2 NP

MAPK have been repeatedly involved in *Nos2* induction and NO production triggered by LPS in macrophages,[35-38] and their role in the synergistic effect of LPS and TiO_2 NP has been investigated (Figure 5). U0126, which prevents the activation of ERK 1/2 by suppressing the activity of the MAP Kinase Kinase MEK1/2,[39] inhibited the increase in NO production caused by exposure to LPS (Panels A and B) and did not hinder, but rather increased the effect of the combined exposure to LPS and TiO_2 NP (Panels C and D). On the contrary, SB203580, which inhibits p38 MAPK catalytic activity by binding to the ATP-binding pocket,[40] was without effect on the stimulation of NO production caused by LPS but partially inhibited the combined effect of TiO_2 NP and LPS. Neither U0126 nor SB203580 affected the slight stimulation of NO production by TiO_2 NP (not shown). Thus, while the ERK1/2 branch appears essential for the stimulation of macrophage NO production by LPS but not by LPS + TiO_2 NP, p38 activation seems more involved in the synergistic effect caused by the combined treatment . Neither ERK1/2 nor p38 are indispensable for the stimulation of NO production by TiO_2 NP.

The role of p38 phosphorylation in the combined effect was directly investigated in the experiment shown in Figure 6. After a short incubation of 3h in the presence of LPS and/or TiO_2 NP, a definite activation of p38 (Panel A) and ERK1/2 (Panel B) was detectable, but the simultaneous exposure to the two compounds showed no additive effect for p38 or a less-than-additive effect for ERK1/2. Conversely, after 6h of treatment, cells co-treated with LPS and TiO_2 NP showed a level of phosphorylated p38 much higher than the cells incubated with either compound alone (Panel A, 6h), while ERK1/2 phosphorylation was comparable in cells treated with LPS or LPS + TiO_2 NP (Panel B, 6h).

3.5 The combined effects of TiO_2 NP and LPS are suppressed by TLR4 inhibition

It is known that LPS is the most important TLR4 ligand and activates macrophages through the transduction pathway triggered by this receptor.[1] The dependence of the effects of NP and LPS on TLR4 is shown in Figure 7. Polymyxin B, an antibiotic derived from *Bacillus polymyxa*, binds the lipid A moiety of LPS with very high affinity, thus preventing its interaction with TLR4.[41] The antibiotic almost completely inhibited the stimulation of NO production (Panel A) or Nos2 protein expression (Panel B) in macrophages treated with TiO_2 NP and LPS, used either alone or together. Polymyxin B had comparable effects on TNFα secretion (Panel C), which was completely suppressed in cells treated with TiO_2 NP, LPS, or both. Also CLI-095, which blocks the signalling mediated by the intracellular domain of TLR4,[42] almost completely suppressed the individual or combined effects of TiO_2 NP and LPS on NO production (Panel D). Polymyxin did not significantly affect the production of NO elicited by treatment with 40 or 80 $\mu g/cm^2$ of NAMA41® (see Fig. 3), indicating that the material was not contaminated with LPS (data not shown).

4. Discussion

In this manuscript, the effects of the simultaneous exposure of macrophages to TiO_2 nanoparticles and LPS are studied. From the data reported in Table 4, the amount of LPS available for the two TiO_2 surfaces is more than one-thousand-fold lower than the saturation level under the experimental conditions adopted. Thus, even if agglomerated in culture medium (Table 3), it is likely that TiO_2 NP bind most if not all the LPS available. Therefore, although it should be expected a higher reactivity for the sample endowed with an higher surface area (NAMA41®), which should be able to drag an higher amount of LPS, the agglomerated state of both materials is expected to decrease the free surface area at comparable levels, and should therefore justify a comparable capacity to adsorb LPS (and, hence, to activate macrophages), consistently with the results obtained.

The endpoints investigated in this study, and found to be synergistically stimulated by TiO_2 NP and LPS, are the increase in NO production and the enhanced secretion of pro-inflammatory cytokines. Both these effects are also involved in the toxicity elicited by TiO_2 NP *in vivo*. In particular, NO increase is responsible for the impairment of microvascular reactivity observed in rats exposed to titania through inhalation.[43-45] Changes in NO production are also of pivotal importance in respiratory pathophysiology: while *Nos2* is constitutively expressed in the human airway epithelium, its expression, along with NO production,[46] is increased by exposure to TiO_2 NP in lung macrophages *in vivo*. Interestingly, recent research supports the use of the non-invasive determination of NO in exhaled breath of workers handling TiO_2 nanopowders as a biomarker of inflammatory effect.[47] As far as cytokines are concerned, their production is observed during lung inflammation caused by TiO_2 after intratracheal instillation[48] or oropharyngeal aspiration.[49] The increased secretion of pro-inflammatory cytokines is also observed after exposure to TiO_2 NP *in vitro.* In particular, the exposure to nanosized TiO_2 stimulates TNF-α secretion in rat alveolar macrophages[15] and in murine macrophages,[50] as well as the secretion of IL-6 in human THP-1 cells, where the co-treatment with LPS potentiate the effect of TiO_2 NP.[51]

TiO_2 NP are increasingly used for industrial purposes and their production is in the order of hundreds of tons per year, although they are considered as relatively non-toxic at the levels detected in occupational settings. On the other hand, the inflammogenic potential of TiO_2 NP *in vivo* has been identified several years ago,[6, 52, 53] and it is known that not only TiO_2 NP, but also carbon-based nanomaterials, [9] significantly exacerbate respiratory inflammation induced by LPS *in vivo*.[54] Those data and the results presented here suggest that, in an occupational setting, a significant part of the inflammatory effects observed may be due not only to nano-structured materials themselves but also to airborne or ground molecules adsorbed therein.[55, 56]

The synergistic effect of LPS and TiO_2 NP on NO production and cytokine secretion, as well as NP internalization, are significantly hampered by cytochalasin D. These data indicate that cytoskeletal integrity and phagocytic activity are required for the effect and point to the involvement of an intracellular site of signalling. On the contrary, consistent with previous literature data[57], the effects of LPS alone on NO production are mostly independent on cytoskeleton, indicating a surface site of signalling.

The MAPK transduction pathway is differently involved in the effects of TiO_2 NP alone or in the presence of LPS. The ERK1/2 branch appears essential for the stimulation of NO production by LPS but not by LPS + TiO_2 NP, while, conversely, p38 seems more involved in the combined effect (Figs. 5 and 6). Interestingly, neither ERK1/2 nor p38 are indispensable for the stimulation of NO production by TiO_2 NP. Previous studies showed that LPS treatment of Raw264.7 cells causes the activation of all the three MAPK pathways, ERK1/2, p38, and JNK.[58,59] Moreover, one of the preparations of TiO_2 NP used here, Aeroxide® P25, triggers MAPK phosphorylation in lung tissue and alveolar macrophages *in vivo*, an effect enhanced by previous priming with LPS.[9] However, it is known that the contribution of the three MAP kinases to *Nos2* induction and NO production by activated macrophages can vary depending upon the macrophage type and the experimental conditions adopted.[35-38] It is therefore, possible, that the simultaneous presence of NP and LPS modulates the MAPK activation pattern, as demonstrated by Liu et al.[60] for gold NP and LPS in the

same cell model used here. In our case, the different sensitivity of the combined and LPS-specific effects to MAPK inhibitors and the clear cut synergy in p38 phosphorylation, observed at 6h of treatment, suggest that the intracellular signals elicited by LPS alone or by LPS and TiO_2 NP are, at least in part, distinct and different.

Moreover, the effects of TiO_2 NP and LPS on *Nos2* induction have also different time courses. Indeed, while the effect of LPS is fairly rapid and is markedly lowered when the treatment is prolonged from 12 h to 24 h, the effect of TiO_2 NP is characterized by a latency of few hours and is larger at 24h than at 6h of treatment. Thus, in the presence of TiO_2 NP, LPS effect is prolonged, and gene induction is still very evident after 24h of treatment (Figure 1B). Also the experiment presented in Fig. 6 indicates that the synergy, as far as p38 phosphorylation is concerned, requires prolonged times of incubation.

Both the effect of LPS alone and the combined effect are abolished if the binding of LPS to TLR4 is prevented by polymyxin B, or the transduction of the TLR4 signal is suppressed by CLI-095. Therefore, the data presented in this contribution suggest that TiO_2 NP enhance the biological activity of LPS in murine macrophages though a mechanism that depends on TLR4, involves the p38 rather than the ERK1/2 branch of the MAPK cascade, and is largely triggered in an intracellular, phagocytosis-dependent compartment. A schematic overview of these signalling pathways are depicted in Figure 8. According to this model, TiO_2 NP would behave as a Trojan horse, able to facilitate the entry of LPS in the endosomal compartment. Thus, when macrophage are exposed simultaneously to LPS and TiO_2 NP, LPS-coated TiO_2 NP cause a quick activation of the plasma membrane TLR4 pathway and promote their endosomal internalization. In this compartment, LPS-TiO_2 NP complexes sustain TLR4-dependent signal transduction leading to enhanced inflammogenic effects.

Conclusions

The findings described in this report demonstrate that the macrophage activation by LPS *in vitro* is markedly enhanced by the simultaneous exposure to TiO_2 NP. The doses of LPS adopted are well below the binding capacity of the TiO_2 NP (Table 4) and suggest that most LPS is bound. Therefore, the overall message of this contribution is that, when bound to TiO_2 NP, LPS exerts a much more powerful inflammatory effect.

This effect may explain why the inflammatory changes observed *in vivo* after exposure to LPS are exacerbated by TiO_2 NP. [9] On the other hand, these results also suggest that the inflammatory changes observed upon exposure to TiO_2 NP may be due, at least in part, to their capability to bind LPS and, possibly, other TLR agonists, thus enhancing the biological activities of these molecules. As a consequence, the inflammatory effects of TiO_2 NP may be of particular concern for individuals with respiratory conditions where increased levels of such compounds are expected.

ACKNOWLEDGMENTS

This work was supported by EU FP7 SANOWORK (Grant n.280716) to EB. Part of the study has been developed during a short traineeship of MA (application UCD-TAF-373), supported by the EU FP7 QNANO project under contract SP4-CAPACITIES-2010-262163.

References

1. Y. Tan and J. C. Kagan, *Mol. Cell*, 2014, 54, 212-223.

2. M. Gangloff, *Trends Biochem. Sci.*, 2012, 37, 92-98.

3. R. C. Lindenschmidt, K. E. Driscoll, M. A. Perkins, J. M. Higgins, J. K. Maurer and K. A. Belfiore, *Toxicol. Appl. Pharmacol.*, 1990, 102, 268-281.

4. H. Shi, R. Magaye, V. Castranova and J. Zhao, *Part. Fibre Toxicol.*, 2013, 10, 15.

5. V. H. Grassian, T. O'Shaughnessy P, A. Adamcakova-Dodd, J. M. Pettibone and P. S. Thorne, *Environ. Health Perspect.*, 2007, 115, 397-402.

6. L. Ma-Hock, S. Burkhardt, V. Strauss, A. O. Gamer, K. Wiench, B. van Ravenzwaay and R. Landsiedel, *Inhal. Toxicol.*, 2009, 21, 102-118.

7. D. Dankovic, E. Kuempel and M. Wheeler, *Inhal. Toxicol.*, 2007, 19 Suppl 1, 205-212.

8. B. van Ravenzwaay, R. Landsiedel, E. Fabian, S. Burkhardt, V. Strauss and L. Ma-Hock, *Toxicol. Lett.*, 2009, 186, 152-159.

9. C. Moon, H. J. Park, Y. H. Choi, E. M. Park, V. Castranova and J. L. Kang, *J. Toxicol. Environ. Health A*, 2010, 73, 396-409.

10. Y. Shi, S. Yadav, F. Wang and H. Wang, *J. Toxicol. Environ. Health A*, 2010, 73, 748-756.

11. M. Yang, K. Flavin, I. Kopf, G. Radics, C. H. Hearnden, G. J. McManus, B. Moran, A. Villalta-Cerdas, L. A. Echegoyen, S. Giordani and E. C. Lavelle, *Small*, 2013, 9, 4194-4206.

12. K. Bhattacharya, M. Davoren, J. Boertz, R. P. Schins, E. Hoffmann and E. Dopp, *Part. Fibre Toxicol.*, 2009, 6, 17.

13. R. K. Shukla, V. Sharma, A. K. Pandey, S. Singh, S. Sultana and A. Dhawan, *Toxicol. In Vitro*, 2011, 25, 231-241.

14. Q. Saquib, A. A. Al-Khedhairy, M. A. Siddiqui, F. M. Abou-Tarboush, A. Azam and J. Musarrat, *Toxicol. In Vitro*, 2012, 26, 351-361.

15. A. M. Scherbart, J. Langer, A. Bushmelev, D. van Berlo, P. Haberzettl, F. J. van Schooten, A. M. Schmidt, C. R. Rose, R. P. Schins and C. Albrecht, *Part. Fibre Toxicol.*, 2011, 8, 31.

16. S. Singh, T. Shi, R. Duffin, C. Albrecht, D. van Berlo, D. Hohr, B. Fubini, G. Martra, I. Fenoglio, P. J. Borm and R. P. Schins, *Toxicol. Appl. Pharmacol.*, 2007, 222, 141-151.

17. S. Hussain, S. Boland, A. Baeza-Squiban, R. Hamel, L. C. Thomassen, J. A. Martens, M. A. Billon-Galland, J. Fleury-Feith, F. Moisan, J. C. Pairon and F. Marano, *Toxicology*, 2009, 260, 142-149.

18. I. Fenoglio, G. Greco, S. Livraghi and B. Fubini, *Chemistry*, 2009, 15, 4614-4621.

19. B. M. Rotoli, O. Bussolati, A. L. Costa, M. Blosi, L. Di Cristo, P. P. Zanello, M. G. Bianchi, R. Visigalli and E. Bergamaschi, *J. Nanopart. Res.*, 2012, 14.

20. G. J. Oostingh, E. Casals, P. Italiani, R. Colognato, R. Stritzinger, J. Ponti, T. Pfaller, Y. Kohl, D. Ooms, F. Favilli, H. Leppens, D. Lucchesi, F. Rossi, I. Nelissen, H. Thielecke, V. F. Puntes, A. Duschl and D. Boraschi, *Part. Fibre Toxicol.*, 2011, 8, 8.

21. P. Ashwood, R. P. Thompson and J. J. Powell, *Exp. Biol. Med. (Maywood)*, 2007, 232, 107-117.

22. T. Hirayama, Y. Tamaki, Y. Takakubo, K. Iwazaki, K. Sasaki, T. Ogino, S. B. Goodman, Y. T. Konttinen and M. Takagi, *J. Orthop. Res.*, 2011, 29, 984-992.

23. W. Jiang, Ph.D. Thesis, University of Massachusetts - Amherst, 2011.

24. S. Smulders, J. P. Kaiser, S. Zuin, K. L. Van Landuyt, L. Golanski, J. Vanoirbeek, P. Wick and P. H. Hoet, *Part. Fibre Toxicol.*, 2012, 9, 41.

25. J. Muller, F. Huaux, N. Moreau, P. Misson, J. F. Heilier, M. Delos, M. Arras, A. Fonseca, J. B. Nagy and D. Lison, *Toxicol. Appl. Pharmacol.*, 2005, 207, 221-231.

26. R. M. German and S. J. Park, *Handbook of mathematical relations in particulate materials processing*, Wiley, New York, 2008.

27. J. O'Brien, I. Wilson, T. Orton and F. Pognan, *Eur. J. Biochem.*, 2000, 267, 5421-5426.

28. S. A. Bustin, *J. Mol. Endocrinol.*, 2000, 25, 169-193.

29. T. P. Misko, R. J. Schilling, D. Salvemini, W. M. Moore and M. G. Currie, *Anal. Biochem.*, 1993, 214, 11-16.

30. T. Preocanin and N. Kallay, *Croat. Chem. Acta*, 2006, 79, 95-106.

31. J. S. Gebauer, M. Malissek, S. Simon, S. K. Knauer, M. Maskos, R. H. Stauber, W. Peukert and L. Treuel, *Langmuir*, 2012, 28, 9673-9679.

32. L. Song, K. Yang, W. Jiang, P. Du and B. S. Xing, *Colloid Surface B*, 2012, 94, 341-346.

33. T. Cedervall, I. Lynch, S. Lindman, T. Berggard, E. Thulin, H. Nilsson, K. A. Dawson and S. Linse, *Proc. Natl. Acad. Sci. USA*, 2007, 104, 2050-2055.

34. J. L. Webb, M. W. Harvey, D. W. Holden and T. J. Evans, *Infect. Immun.*, 2001, 69, 6391-6400.

35. C. C. Chen and J. K. Wang, *Mol. Pharmacol.*, 1999, 55, 481-488.

36. K. M. Rao, T. Meighan and L. Bowman, *J. Toxicol. Environ. Health A*, 2002, 65, 757-768.

37. J. W. Kim and C. Kim, *Biochem. Pharmacol.*, 2005, 70, 1352-1360.

38. E. Jones, I. M. Adcock, B. Y. Ahmed and N. A. Punchard, *J. Inflamm. (Lond)*, 2007, 4, 23.

39. D. R. DeSilva, E. A. Jones, M. F. Favata, B. D. Jaffee, R. L. Magolda, J. M. Trzaskos and P. A. Scherle, *J. Immunol.*, 1998, 160, 4175-4181.

40. S. Kumar, M. S. Jiang, J. L. Adams and J. C. Lee, *Biochem. Biophys. Res. Commun.*, 1999, 263, 825-831.

41. R. A. Moore, N. C. Bates and R. E. Hancock, *Antimicrob. Agents Chemother.*, 1986, 29, 496-500.

42. M. Ii, N. Matsunaga, K. Hazeki, K. Nakamura, K. Takashima, T. Seya, O. Hazeki, T. Kitazaki and Y. Iizawa, *Mol. Pharmacol.*, 2006, 69, 1288-1295.

43. A. J. LeBlanc, J. L. Cumpston, B. T. Chen, D. Frazer, V. Castranova and T. R. Nurkiewicz, *J. Toxicol. Environ. Health A*, 2009, 72, 1576-1584.

44. A. J. LeBlanc, A. M. Moseley, B. T. Chen, D. Frazer, V. Castranova and T. R. Nurkiewicz, *Cardiovasc. Toxicol.*, 2010, 10, 27-36.

45. T. L. Knuckles, J. Yi, D. G. Frazer, H. D. Leonard, B. T. Chen, V. Castranova and T. R. Nurkiewicz, *Nanotoxicology*, 2012, 6, 724-735.

46. R. Liu, X. Zhang, Y. Pu, L. Yin, Y. Li, G. Liang, X. Li and J. Zhang, *J. Nanosci. Nanotechnol.*, 2010, 10, 5161-5169.

47. W. T. Wu, H. Y. Liao, Y. T. Chung, W. F. Li, T. C. Tsou, L. A. Li, M. H. Lin, J. J. Ho, T. N. Wu and S. H. Liou, *Int. J. Mol. Sci.*, 2014, 15, 878-894.

48. A. Gustafsson, E. Lindstedt, L. S. Elfsmark and A. Bucht, *J. Immunotoxicol.*, 2011, 8, 111-121.

49. N. L. Delgado-Buenrostro, E. I. Medina-Reyes, I. Lastres-Becker, V. Freyre-Fonseca, Z. Ji, R. Hernandez-Pando, B. Marquina, J. Pedraza-Chaverri, S. Espada, A. Cuadrado and Y. I. Chirino, *Environ. Toxicol.*, 2014, doi: 10.1002/tox.21957.

50. S. Xiong, S. George, H. Yu, R. Damoiseaux, B. France, K. W. Ng and J. S. Loo, *Arch. Toxicol.*, 2013, 87, 1075-1086.

51. T. Morishige, Y. Yoshioka, A. Tanabe, X. Yao, S. Tsunoda, Y. Tsutsumi, Y. Mukai, N. Okada and S. Nakagawa, *Biochem. Biophys. Res. Commun.*, 2010, 392, 160-165.

52. G. Oberdorster, J. N. Finkelstein, C. Johnston, R. Gelein, C. Cox, R. Baggs and A. C. Elder, *Res. Rep. Health Eff. Inst.*, 2000, 5-74.

53. N. Kobayashi, M. Naya, S. Endoh, J. Maru, K. Yamamoto and J. Nakanishi, *Toxicology*, 2009, 264, 110-118.

54. K. Inoue, *Environ. Health Prev. Med.*, 2011, 16, 139-143.

55. C. M. Long, H. H. Suh, L. Kobzik, P. J. Catalano, Y. Y. Ning and P. Koutrakis, *Environ. Health Perspect.*, 2001, 109, 1019-1026.

56. J. M. Soukup and S. Becker, *Toxicol. Appl. Pharmacol.*, 2001, 171, 20-26.

57. S. M. Eswarappa, V. Pareek and D. Chakravortty, *Innate Immun.*, 2008, 14, 309-318.

58. J. S. Sanghera, S. L. Weinstein, M. Aluwalia, J. Girn and S. L. Pelech, *J. Immunol.*, 1996, 156, 4457-4465.

59. S. Akira and K. Takeda, *Nat. Rev. Immunol.*, 2004, 4, 499-511.

60. Z. Liu, W. Li, F. Wang, C. Sun, L. Wang, J. Wang and F. Sun, *Nanoscale*, 2012, 4, 7135-7142.

Table 1.

Primers and temperatures of annealing adopted for RT-PCR experiments

Gene	Protein	Forward	Reverse	T (°C)	Amplicon size (bp)
Inducible Nitric oxide synthetase *(Nos2)*	Inducible Nitric oxide synthetase (Nos2)	5'-GTT CTC AGC CCA ACA ATA CAA GA-3'	5'-GTG GAC GGG TCG ATG TCA C-3'	57°C	127
Prostaglandin-endoperoxidesynthase 2 *(Ptgs2)*	Cyclooxygenase-2 (Cox2)	5'-GCTCAGCCAG GCAGCAAATC -3'	5'-ATCCAGTCCG GGTACAGTCA-3'	56°C	107
Glyceraldehyde 3-phosphate dehydrogenase*(Gapdh)*	Glyceraldehyde 3-phosphate dehydrogenase	5'-TGT TCC TAC CCC CAA TGT GT-3'	5'-GGT CCT CAG TGT AGC CCA AG-3'	57°C	137

Table 2. Physico-chemical properties of NAMA41® (spray dried) and Aeroxide® P25

TiO_2 NP	XRD phase distribution		Density (g/cm^3)	SSA_{BET}* (m^2/g)	d_{BET}** (nm)
	Anatase (%)	B = Brookite, R = Rutile, (%)			
NAMA41®	84	16, B	3,98	154	10
Aeroxide® P25	83	17, R	4,10	60	24

Table 3. Mean size distribution by intensity and ζ potential for 0.125 mg/ml of NAMA41® and Aeroxide® P25 dispersed in deionized water and complete culture medium.

TiO_2 NP	Deionized water$_{natural\ pH}$				Deionized water$_{medium\ pH}$				Complete culture medium			
	pH	Size (d. nm)	PdI#	ζ pot. (mV)	pH	Size (d. nm)	PdI#	ζ pot. (mV)	pH	Size (d. nm)	PdI#	ζ pot. (mV)
NAMA41®	3.9	45	0.48	41.2	7.3	9864	0.76	-15.9	7.3	1962	0.98	-10.9
S.D.		1	0.09	0.0		2390	0.30	0.4		147	0.03	0.5
Aeroxide P25®	6.5	286	0.30	37.4	7.7	3425	0.36	-11.0	7.7	532	0.53	-10.8
S.D.		4	0.04	0.9		226	0.10	0.1		16	0.11	0.4

 # PDI: Polydispersity Index

Table 4. Amount of BSA and LPS present in test samples, normalized for the TiO_2 NP surface area.

TiO_2 NP	SSA (m^2/g)	BSA/TiO_2* (mg/m^2)	LPS/TiO_2 (mg/m^2)**
NAMA41®	154	25.4	0.00005
Aeroxide P25®	60	65.1	0.00013

*** referred to a BSA concentration of 0.05%.**

**** referred to a LPS concentration of 1 ng/ml.**

Legends to figures

Figure 1

Effects of TiO_2 NP and LPS on *Nos2* expression and NO production in Raw264.7 cells. Growth medium was replaced 24h after cell seeding with medium supplemented with the indicated doses of TiO_2 NP and/or LPS. A. After 24h of treatment, mRNA was extracted and the expression of *Nos2* evaluated as described in Experimental. Data are means ± S.D. of four independent determinations in two separate experiments. *p<0.05 *vs.* control, untreated cultures; ###p<0.001 *vs.* cultures treated with LPS 1 ng/ml alone; $p<0.05 *vs*. LPS 10 ng/ml alone. B. At the indicated times, cells were lysed and the expression of *Nos2* mRNA was evaluated through RT-PCR. Data are expressed as fold stimulation *vs.* control, untreated cells and are means of 4 determinations ± S.D. obtained in two separate experiments. *p< 0.05, **p<0.01,***p<0.001 *vs.* the same experimental condition at 6h of treatment; #p<0.05, ##p<0.01, ###p<0.001 .*vs.* the same experimental condition at 12h of treatment. C. After 48h of treatment, cells were extracted, and the expression of the protein Nos2 was evaluated through Western Blot. A representative blot is shown, with actin expression used for loading control (upper panel). In the lower panel the densitometric analysis of Nos2 protein is shown. D. After 48h of treatment, nitrite concentration was determined in the culture medium. Data are means of eight independent determinations ± S.D. in two separate experiments. **p<0.01, ***p<0.001 *vs.* control, untreated cultures; ##p<0.001 *vs.* cultures treated with LPS 1 ng/ml alone; $$p<0.01 *vs*. LPS 10 ng/ml alone.

Figure 2

Synergistic effects of TiO_2 NP and LPS on the expression of inflammatory markers. A. Growth medium was replaced 24h after cell seeding with medium supplemented with the indicated doses of TiO_2 NP and/or LPS. A. After 24h of treatment, mRNA was extracted and the expression of *Ptgs2*

was analyzed with RT-PCR. Data are means of 4 independent determinations in two separate experiments with S.D. indicated. B, C. After 48h of treatment, TNF-α (Panel B) and IL-6 (Panel C) were determined in the extracellular medium, as described under Experimental. Data are means of 3 independent determinations ± S.D. For A, B, and C *p<0.05, ***p<0.001 *vs.* control, untreated cultures; ##p<0.01, ###p<0.001 *vs.* cultures treated with LPS 1 ng/ml alone; $p<0.05, $$$p<0.001 *vs*. LPS 10 ng/ml alone.

Figure 3

Effects of two preparations of TiO_2 NP on inflammatory markers in Raw264.7 cells. Growth medium was replaced 24h after cell seeding with medium supplemented with the indicated additives. A. After 48h of treatment, nitrite concentration was determined in the culture medium. Data are means of eight independent determinations ± S.D. in two separate experiments. **p<0.01, ***p<0.001 *vs.* control, untreated cultures; #p<0.05, ###p<0.001 *vs.* cultures treated with LPS 1 ng/ml alone, as evaluated by two-way ANOVA for multiple comparisons with Tukey correction. B. After 24h of treatment, mRNA was extracted and the expression of *Nos2* evaluated as described in Experimental. Data are means ± S.D. of four independent determinations in two separate experiments. *p<0.05, **p<0.01 *vs.* control, untreated cultures; ###p<0.001 *vs.* cultures treated with LPS 1 ng/ml alone. C. After 48h of treatment, TNF-α was determined in the extracellular medium, as described under Experimental. Data are means of 3 independent determinations ± S.D. **p<0.01, ***p<0.001 *vs.* control, untreated cultures; ###p<0.001 *vs.* cultures treated with LPS 1 ng/ml alone.

Figure 4

Effects of cytochalasin B on NO production and NP internalization by Raw264.7 cells treated with TiO_2 NP and LPS. Cells were treated as described in Figure 1D. One hour before exposure to TiO_2 NP (80 μg/cm^2) and/or LPS (1 ng/ml or 10 ng/ml), cytochalasin B (5 μg/ml) was added to the

medium, as indicated, and maintained throughout the experimental treatment. A. After 48h, nitrite concentration was determined in the extracellular medium, as described under Experimental. Data are means of four independent determinations ± S.D. *p<0.05, **p<0.01,***p<0.001 *vs.* control, untreated cultures; ###p<0.001 *vs.* cultures treated under the same conditions without the inhibitor. B, C. Parallel cultures were seeded on coverslides and incubated for 24h with TiO_2 NP (10 μg/cm^2) in the presence of LPS (1 ng/ml), without (B) or with (C) cytochalasin B. At the end of the experiment cells were labelled and fixed as detailed under Experimental. For either condition, a single horizontal confocal section is shown along with two orthogonal projections. Dashed lines highlight the orthogonal projections of single cells. White, TiO_2 NP; Blue, nuclei; Red, cytoplasm. Images report representative fields. Bar = 20 μm.

Figure 5

Differential effects of MAPK inhibitors on NO production promoted by TiO_2 NP and LPS. Cells were treated as described in Figure 1D. A,B,C,D. One hour before the exposure, the MAPK inhibitors U0126 or SB203580 were added to the medium, as indicated, and maintained throughout the experimental treatment. After 48h of treatment, nitrite concentration was determined in the extracellular medium, as described under Experimental. Data are expressed as percent of the value obtained under the indicated conditions in the absence of inhibitors and are means of eight independent determinations ± S.D. Statistical analysis was performed on the absolute values. For all the panels, **p<0.01 and ***p<0.001 *vs.* cultures incubated with the same doses of LPS and TiO_2 NP in the absence of inhibitors.

Figure 6

The synergistic effect of LPS and TiO_2 NPs on p38 phosphorylation. Cells were incubated for 3h or 6h in the presence of LPS and/or TiO_2 NP. At the indicated times cells were lysed and the

expression of the phosphorylated isoform and of total p38 (Panels A) or ERK1/2 (Panels B) was assessed. Tubulin was used as loading control. In the lower part of each panel the densitometric analysis is shown. The experiment was performed twice with comparable results.

Figure 7

Effects of TLR4 inhibitors on NO and TNF-α production by Raw264.7 cells treated with TiO_2 NP and LPS. Cells were treated as described in Figure 2. One hour before exposure to TiO_2 NP (80 $\mu g/cm^2$) and/or LPS (1 ng/ml or 10 ng/ml), polymyxin B or CLI-095 were added to the incubation medium, as indicated, and maintained throughout the experimental treatment. After 48h, the concentration of nitrites (Panels A and D), the expression of Nos2 (Panel B) and the secretion of TNF-α (Panel C) were determined, as described under Experimental. For B, a representative experiment is shown, performed twice with comparable results. Data are means (n = 4 for A and D, n = 3 for C) ± S.D. in a representative experiment. *$p<0.05$, **$p<0.01$,***$p<0.001$ *vs.* control, untreated cultures; #$p<0.05$, ##$p<0.01$, ### $p<0.001$ *vs.* cultures treated under the same conditions without the inhibitor.

Figure 8

A comparison between the transduction pathways triggered by LPS alone (left) and by LPS + TiO_2 NP (right). See text for further explanations.

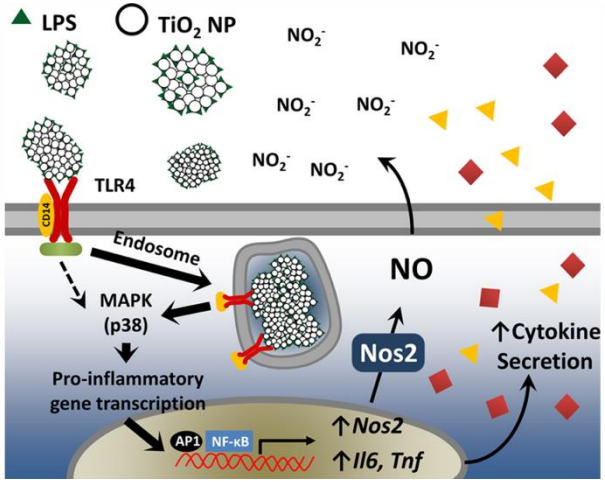

TiO_2 nanoparticles enhance LPS-dependent NO production and the induction of pro-inflammatory genes through a mechanism requiring TLR4 and cytoskeletal integrity

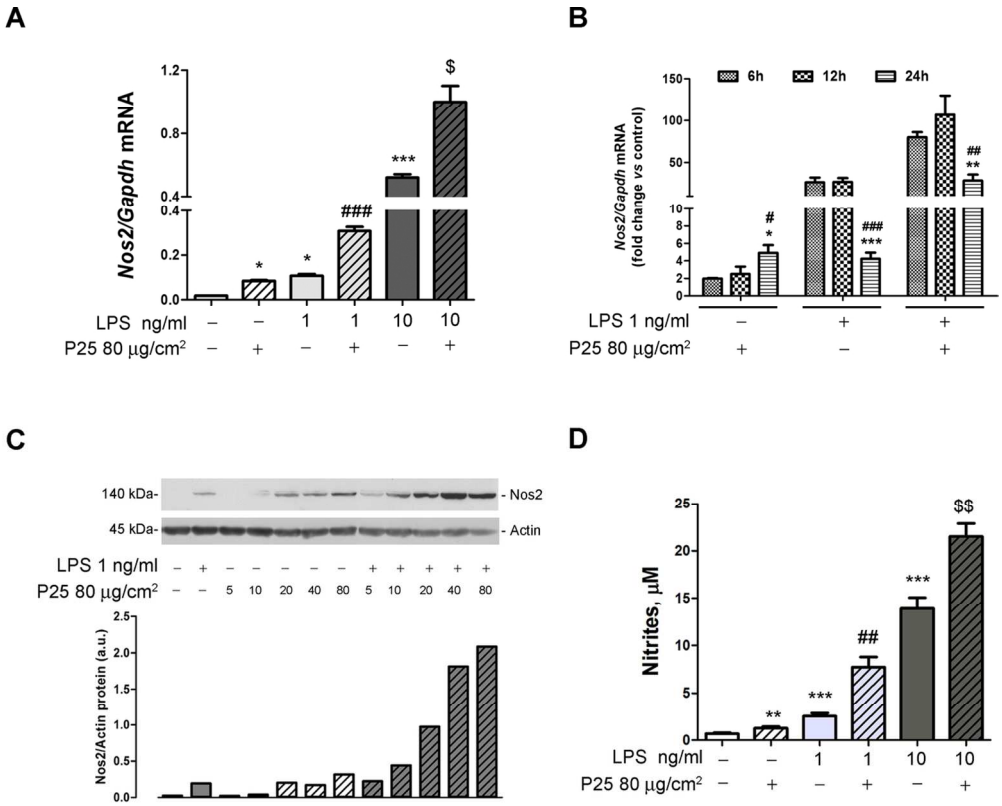

Figure 1
Effects of TiO_2 NP and LPS on *Nos2* expression and NO production in Raw264.7 cells. Growth medium was replaced 24h after cell seeding with medium supplemented with the indicated doses of TiO_2 NP and/or LPS. A. After 24h of treatment, mRNA was extracted and the expression of *Nos2* evaluated as described in Experimental. Data are means ± S.D. of four independent determinations in two separate experiments. *p<0.05 *vs.* control, untreated cultures; ###p<0.001 *vs.* cultures treated with LPS 1 ng/ml alone; $p<0.05 *vs.* LPS 10 ng/ml alone. B. At the indicated times, cells were lysed and the expression of *Nos2* mRNA was evaluated through RT-PCR. Data are expressed as fold stimulation *vs.* control, untreated cells and are means of 4 determinations ± S.D. obtained in two separate experiments. *p< 0.05, **p<0.01,***p<0.001 *vs.* the same experimental condition at 6h of treatment; #p<0.05, ##p<0.01, ###p<0.001 *vs.* the same experimental condition at 12h of treatment. C. After 48h of treatment, cells were extracted, and the expression of the protein Nos2 was evaluated through Western Blot. A representative blot is shown, with actin expression used for loading control (upper panel). In the lower panel the densitometric analysis of Nos2 protein is shown. D. After 48h of treatment, nitrite concentration was determined in the culture medium. Data are means of eight independent determinations ± S.D. in two separate experiments. **p<0.01, ***p<0.001 *vs.* control, untreated cultures; ##p<0.001 *vs.* cultures treated with LPS 1 ng/ml alone; $$p<0.01 *vs.* LPS 10 ng/ml alone.
120x95mm (300 x 300 DPI)

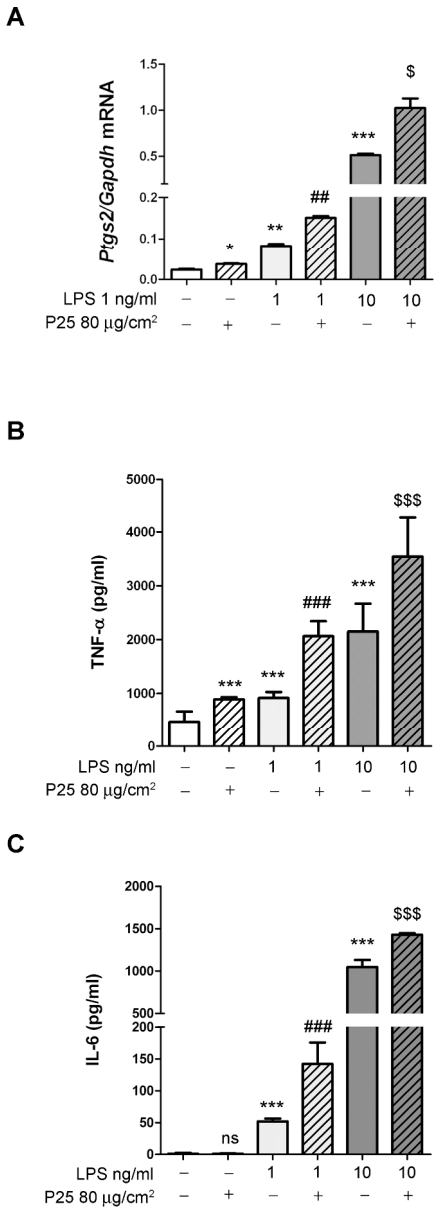

Figure 2
Synergistic effects of TiO_2 NP and LPS on the expression of inflammatory markers. A. Growth medium was replaced 24h after cell seeding with medium supplemented with the indicated doses of TiO_2 NP and/or LPS. A. After 24h of treatment, mRNA was extracted and the expression of *Ptgs2* was analyzed with RT-PCR. Data are means of 4 independent determinations in two separate experiments with ± S.D. indicated. B, C. After 48h of treatment, TNF-α (Panel B) and IL-6 (Panel C) were determined in the extracellular medium, as described under Experimental. Data are means of 3 independent determinations ± S.D. For A, B, and C *p<0.05, ***p<0.001 *vs.* control, untreated cultures; ##p<0.01, ###p<0.001 *vs.* cultures treated with LPS 1 ng/ml alone; $p<0.05, $$$p<0.001 *vs.* LPS 10 ng/ml alone.
200x561mm (300 x 300 DPI)

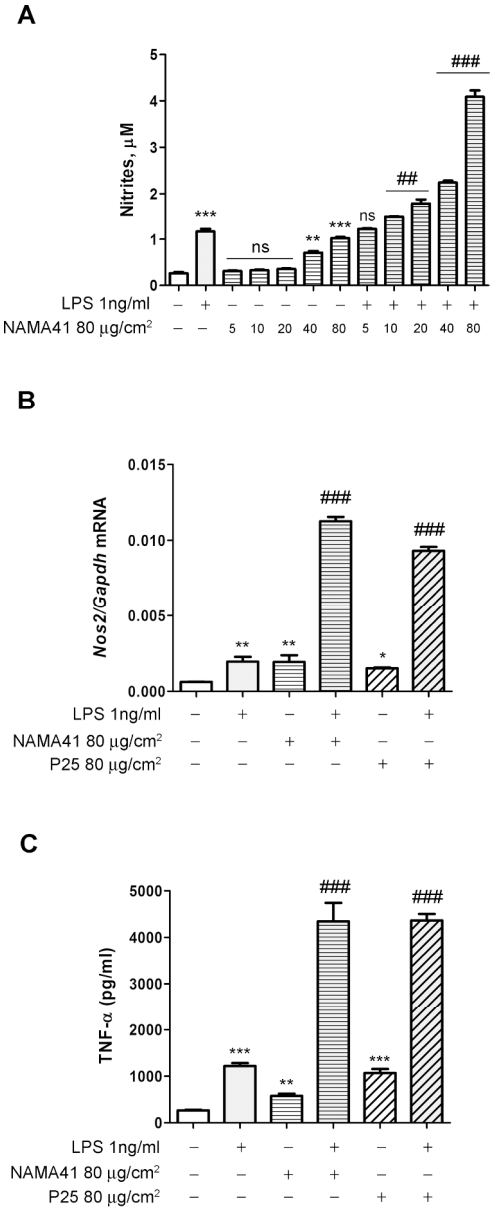

Figure 3
Effects of two preparations of TiO_2 NP on inflammatory markers in Raw264.7 cells. Growth medium was replaced 24h after cell seeding with medium supplemented with the indicated additives. A. After 48h of treatment, nitrite concentration was determined in the culture medium. Data are means of eight independent determinations ± S.D. in two separate experiments. **p<0.01, ***p<0.001 *vs.* control, untreated cultures; #p<0.05, ###p<0.001 *vs.* cultures treated with LPS 1 ng/ml alone, as evaluated by two-way ANOVA for multiple comparisons with Tukey correction. B. After 24h of treatment, mRNA was extracted and the expression of *Nos2* evaluated as described in Experimental. Data are means ± S.D. of four independent determinations in two separate experiments. *p<0.05, **p<0.01 *vs.* control, untreated cultures; ###p<0.001 *vs.* cultures treated with LPS 1 ng/ml alone. C. After 48h of treatment, TNF-α was determined in the extracellular medium, as described under Experimental. Data are means of 3 independent determinations ± S.D. **p<0.01, ***p<0.001 *vs.* control, untreated cultures; ###p<0.001 *vs.* cultures treated with LPS 1 ng/ml alone.

197x488mm (300 x 300 DPI)

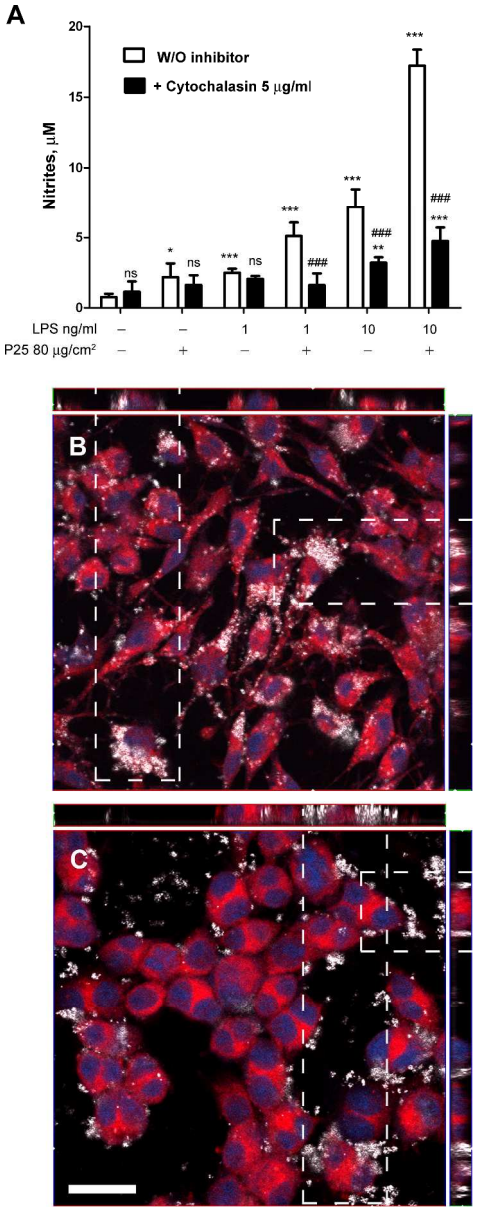

Figure 4
Effects of cytochalasin B on NO production and NP internalization by Raw264.7 cells treated with TiO_2 NP and LPS. Cells were treated as described in Figure 1D. One hour before exposure to TiO_2 NP (80 μg/cm^2) and/or LPS (1 ng/ml or 10 ng/ml), cytochalasin B (5 μg/ml) was added to the medium, as indicated, and maintained throughout the experimental treatment. A. After 48h, nitrite concentration was determined in the extracellular medium, as described under Experimental. Data are means of four independent determinations ± S.D. *p<0.05, **p<0.01,***p<0.001 *vs.* control, untreated cultures; ###p<0.001 *vs.* cultures treated under the same conditions without the inhibitor. B, C. Parallel cultures were seeded on coverslides and incubated for 24h with TiO_2 NP (10 μg/cm^2) in the presence of LPS (1 ng/ml), without (B) or with (C) cytochalasin B. At the end of the experiment cells were labelled and fixed as detailed under Experimental. For either condition, a single horizontal confocal section is shown along with two orthogonal projections. Dashed lines highlight the orthogonal projections of single cells. White, TiO_2 NP; Blue, nuclei; Red, cytoplasm. Images report representative fields. Bar = 20 μm.

389x999mm (300 x 300 DPI)

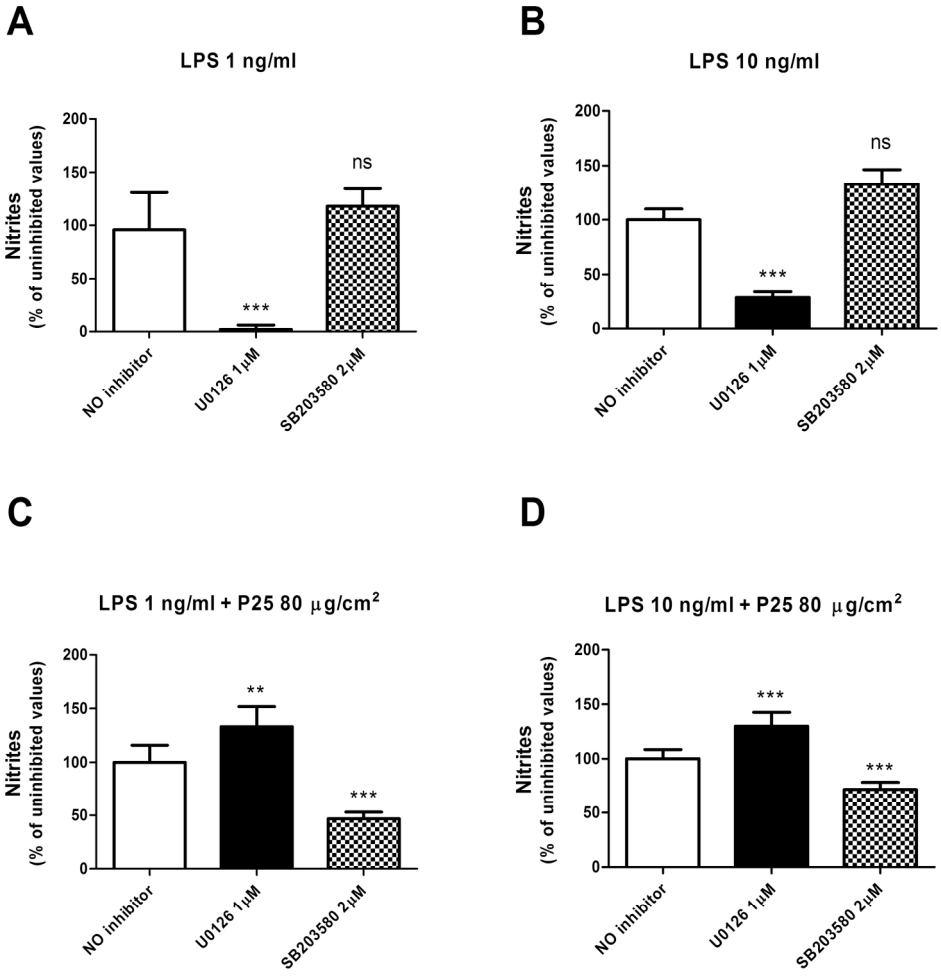

Figure 5
Differential effects of MAPK inhibitors on NO production promoted by TiO_2 NP and LPS. Cells were treated as described in Figure 1D. A,B,C,D. One hour before the exposure, the MAPK inhibitors U0126 or SB203580 were added to the medium, as indicated, and maintained throughout the experimental treatment. After 48h of treatment, nitrite concentration was determined in the extracellular medium, as described under Experimental. Data are expressed as percent of the value obtained under the indicated conditions in the absence of inhibitors and are means of eight independent determinations ± S.D. Statistical analysis was performed on the absolute values. For all the panels, **$p<0.01$ and ***$p<0.001$ *vs.* cultures incubated with the same doses of LPS and TiO_2 NP in the absence of inhibitors.

182x187mm (300 x 300 DPI)

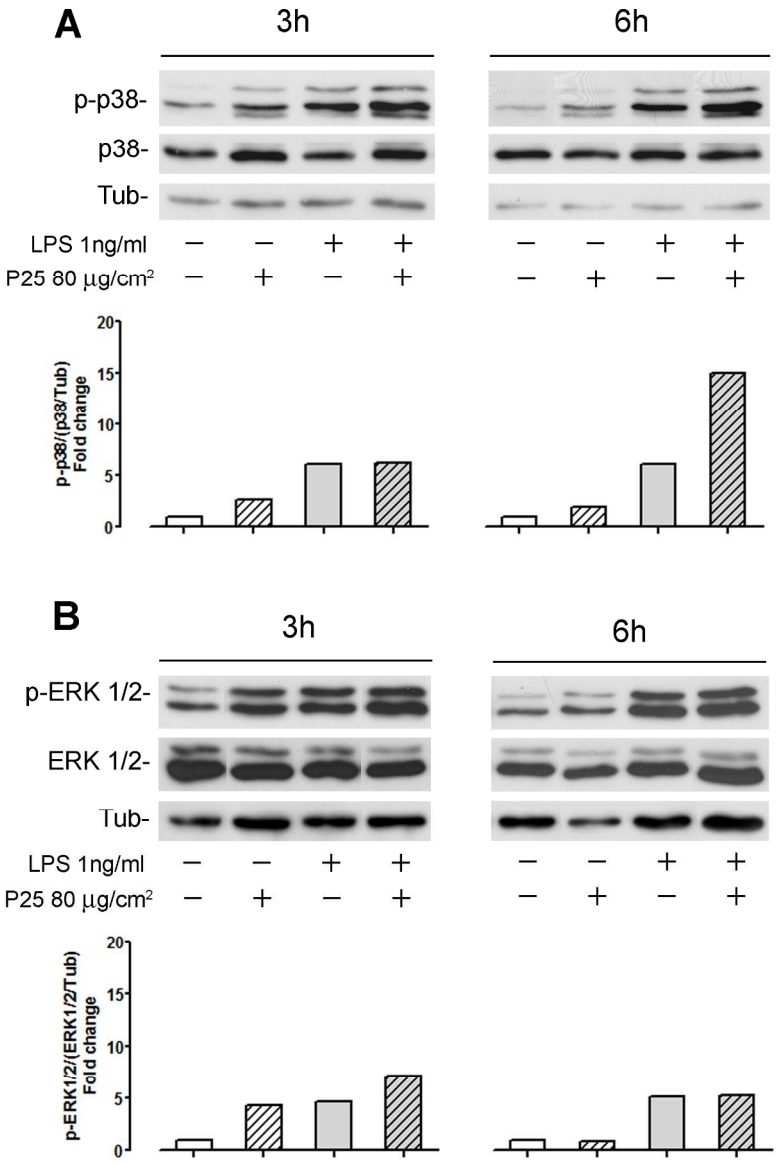

Figure 6
The synergistic effect of LPS and TiO_2 NP on p38 phosphorylation. Cells were incubated for 3h or 6h in the presence of LPS and/or TiO_2 NP. At the indicated times cells were lysed and the expression of the phosphorylated isoform and of total p38 (Panels A and B) or ERK1/2 (Panels C and D) was assessed. Tubulin was used as loading control. In the lower part of each panel the densitometric analysis is shown. The experiment was performed twice with comparable results.

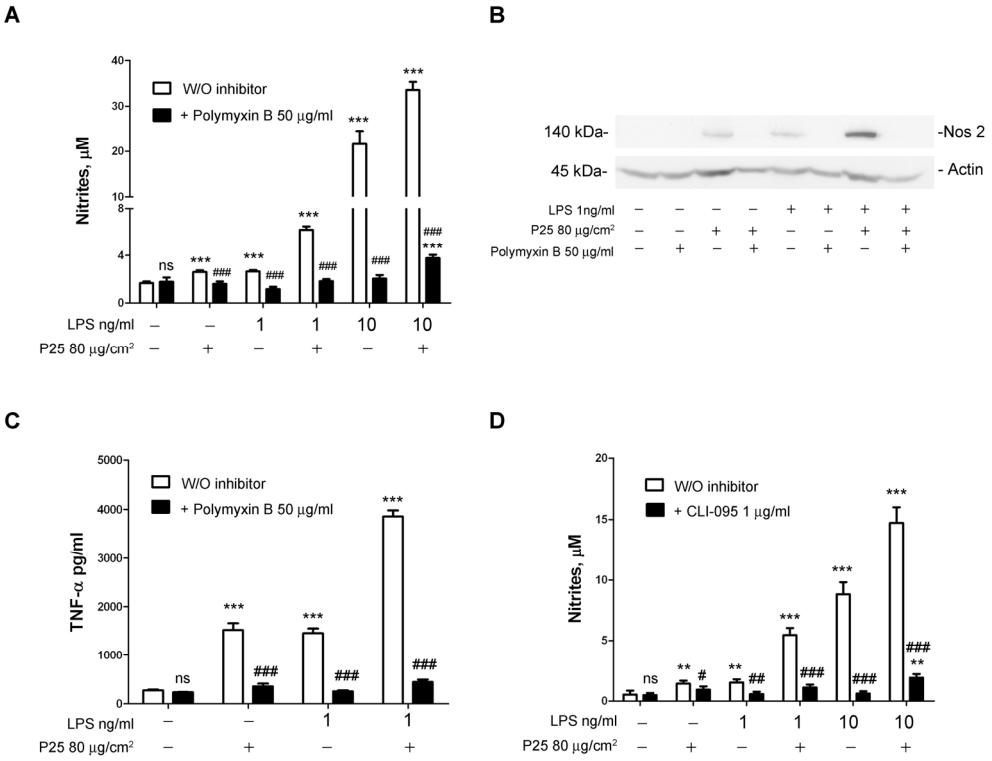

Figure 7
Effects of TLR4 inhibitors on NO and TNF-α production by Raw264.7 cells treated with TiO_2 NP and LPS. Cells were treated as described in Figure 2. One hour before exposure to TiO_2 NP (80 μg/cm^2) and/or LPS (1 ng/ml or 10 ng/ml), polymyxin B or CLI-095 were added to the incubation medium, as indicated, and maintained throughout the experimental treatment. After 48h, the concentration of nitrites (Panels A and D), the expression of Nos2 (Panel B) and the secretion of TNF-α (Panel C) were determined, as described under Experimental. For B, a representative experiment is shown, performed twice with comparable results. Data are means (n = 4 for A and D, n = 3 for C) ± S.D. in a representative experiment. *p<0.05, **p<0.01,***p<0.001 *vs.* control, untreated cultures; #p<0.05, ##p<0.01, ### p<0.001 *vs.* cultures treated under the same conditions without the inhibitor.

179x147mm (300 x 300 DPI)

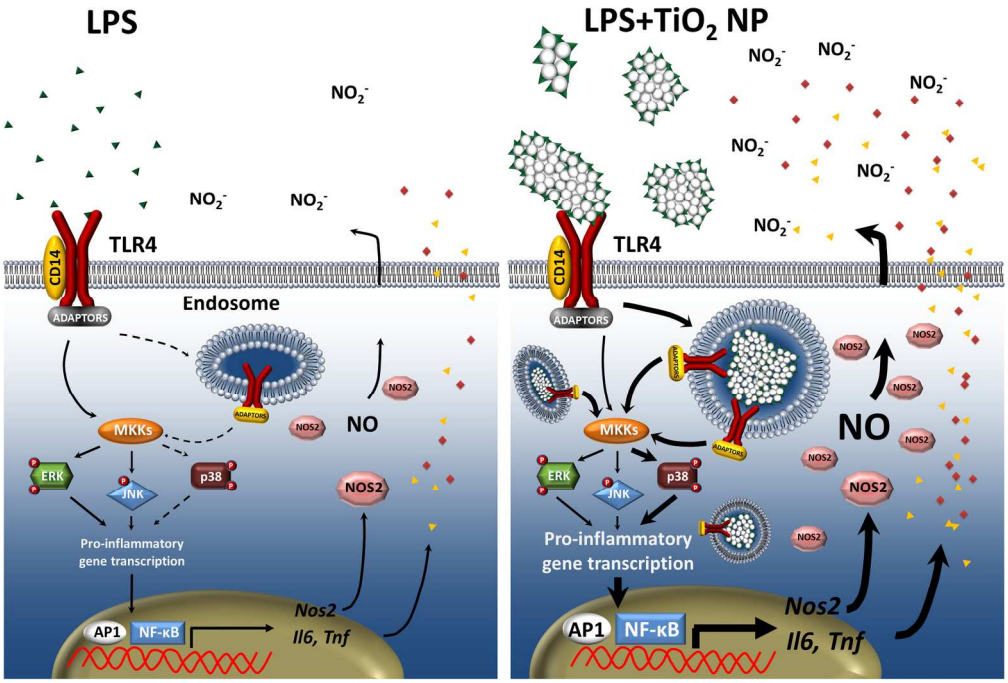

Figure 8
A comparison between the transduction pathways triggered by LPS alone (left) and by LPS + TiO_2 NP (right).
See text for further explanations.
107x72mm (600 x 600 DPI)

Supplementary Material

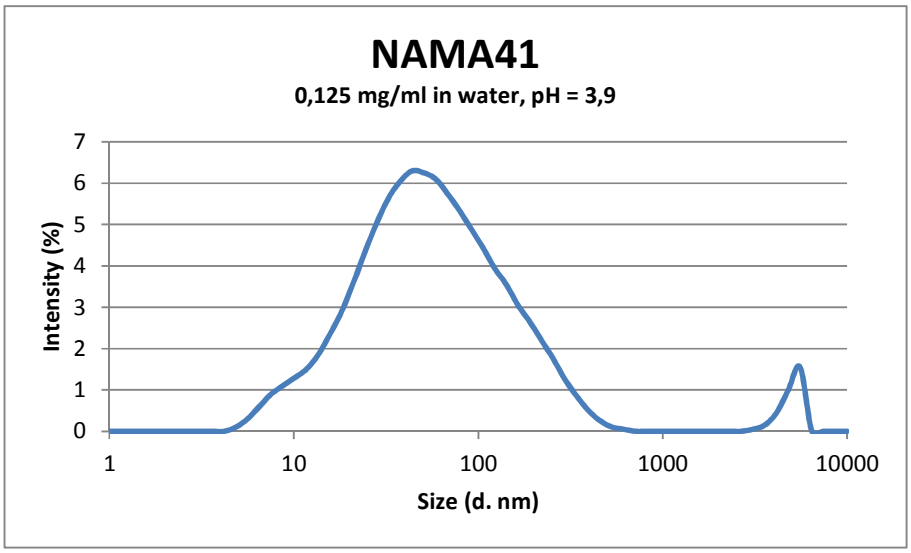

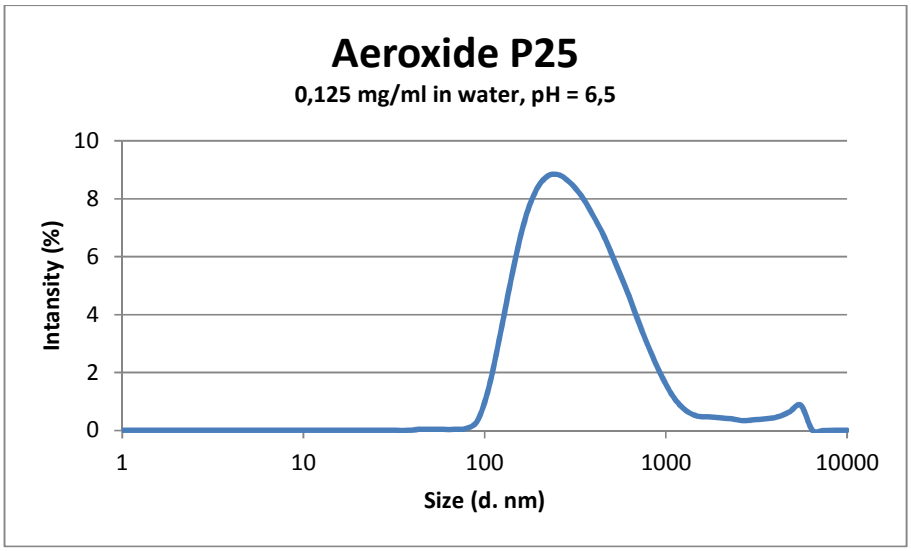

Figure S1

DLS particle size distribution by Intensity for NAMA 41 and Aeroxide P25 in deionized water.

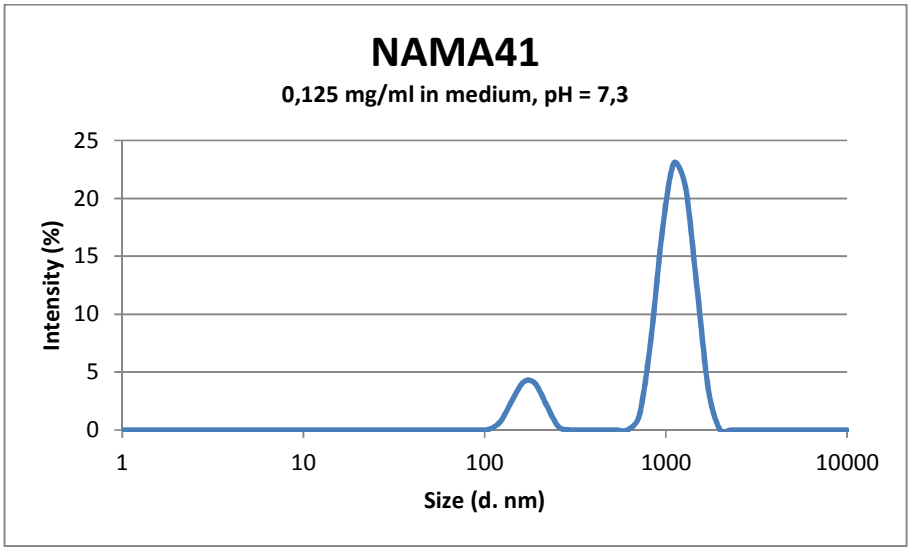

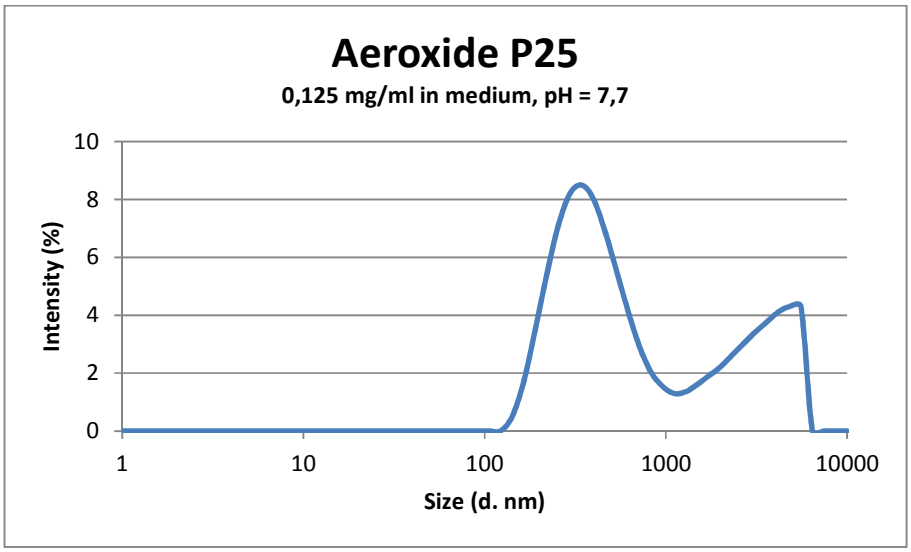

Figure S2

DLS particle size distribution by Intensity for NAMA 41 and Aeroxide P25 in complete culture medium.

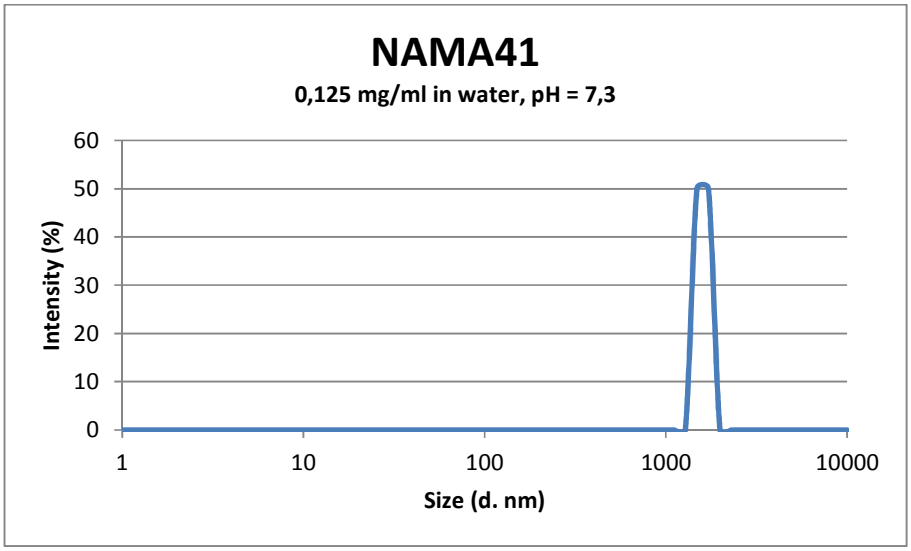

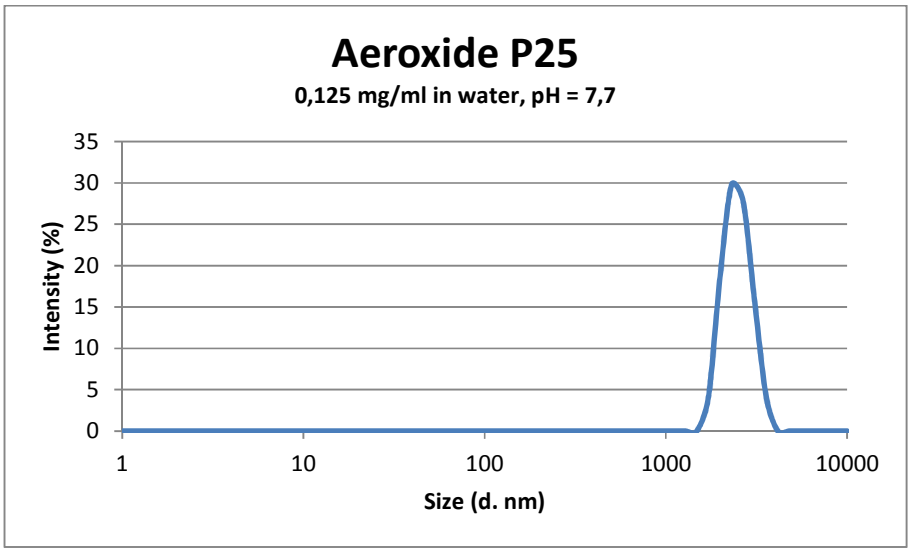

Figure S3

DLS particle size distribution by Intensity for NAMA 41 and Aeroxide P25 in deionized water at medium pH.

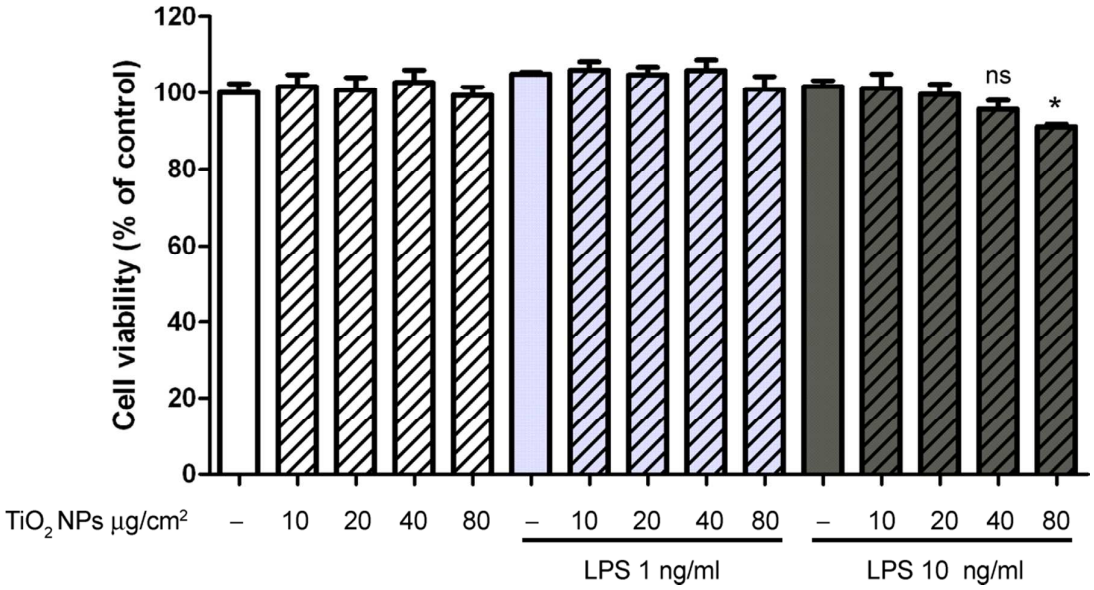

Figure S4

Cell viability of Raw264.7 cells after treatment with TiO_2 NP alone or in combination with LPS. Growth medium was replaced 24h after cell seeding with medium supplemented with TiO_2 NP in a dose range from 10 to 80 µg/cm^2 in the presence or in the absence of LPS 1ng/ml or 10 ng/ml. After 48 h, cell viability was determined with the resazurin assay (see Experimental). Data are means of four independent experimental runs ± S.D. *$p<0.05$. ns = not significant *vs.* control, untreated cells.